Marine and Petroleum Geology 140 (2022) 105661

Contents lists available at ScienceDirect

Marine and Petroleum Geology

journal homepage: www.elsevier.com/locate/marpetgeo

Controls on and geological models of hydrocarbon accumulation in gentle slopes caused by exceptionally weak tectonic activities: A case study of the Lixian Slope, Raoyang Sag, Eastern China

Fugui He [a,b], Xianzhi Gao [a,*], Dexiang Yang [c], Bingda Fan [c], Changqing Ren [a,b,d], Huiping Guo [c], Huilai Wang [c], Yuanxin Huang [c]

[a] College of Geosciences, China University of Petroleum, Beijing, 102249, China
[b] State Key Laboratory of Organic Geochemistry, Guangzhou Institute of Geochemistry, Chinese Academy of Sciences, Guangzhou, 510640, China
[c] Exploration and Development Institute of Huabei Oilfield Branch Company, PetroChina, Renqiu, Hebei, 062550, China
[d] School of Earth Science and Engineering, Hebei University of Engineering, Handan, Hebei, 056038, China

ARTICLE INFO

Keywords:
Lixian slope
Weak tectonic activity
Fault
Connectivity of sandbody
Controls on hydrocarbon accumulation
Hydrocarbon accumulation model

ABSTRACT

The Lixian Slope is located in the western part of the Raoyang Sag, Bohai Bay Basin, Northern China. This slope was developed due to exceptionally weak tectonic activities; therefore, it is aptly called a weak tectonic slope. The slope gradients, faults, sandbodies, source rocks, and oil-source correlation were evaluated. During the development of the Lixian Slope, its gradients were usually low (generally less than 1.00°). Most of the faults have low fault throws (usually less than 30 m). Moreover, the faults of this slope have poor vertical transporting capacity. The sandstone-to-strata ratios for different Paleogene strata of the Lixian Slope are generally less than 40%, suggesting that the connectivity of sandbodies in the Paleogene strata is poor. In addition, research on the sources of crude oil indicates that the oil in most slope areas originated from Es1x source rocks. The study of the controls on hydrocarbon accumulation in the Lixian Slope indicates the following: 1) the planar distribution of oil and gas reservoirs in the Lixian Slope is strictly controlled by both the Es1x and Ek–Es4 source rocks, the Es1x in particular; 2) the sandbodies, faults, and low gradients control the planar enrichment of hydrocarbons; and 3) the faults and source rocks control the vertical distribution of oil and gas reservoirs. According to the characteristics of and controls on hydrocarbon accumulation, a hydrocarbon accumulation model suitable for a weak tectonic slope is proposed. Finally, a few recommendations for future explorations are suggested. The Es2 and Es1 members, especially those near the NNE–NEE trending faults, are critical target intervals for future exploration operations.

1. Introduction

The Lixian Slope is a gentle slope belt (Ren, 2009). A gentle slope belt, a part of a fault sag (or fault basin), is a secondary structural belt connecting the surrounding uplift and a trough at a relatively low gradient (Li et al., 2003; Zhang, 2006). Fault–sags, such as the Shulu Sag, Baxian Sag, and Cuddapah Sag, are widely developed globally (Zhao et al., 2012; Basu et al., 2021). In China, fault–sags are mainly found in the eastern coastal regions from Hainan to Liaoning (Li et al., 2003; Zhao et al., 2012). The gentle slope lies adjacent to the trough in which the source rocks have been developed and located higher than the trough. Thus, these cause the oil and gas, expulsed by the source rocks, to migrate toward the gentle slope. Generally, these oils and gases can migrate from the trough to the outer slope for long distances. The distribution of oil and gas in a gentle slope depends mainly on the distribution characteristics of effective source rocks and the structural characteristics of the slope, especially the latter. When a gentle slope is characterized by weak terrain deformations, the oil and gas will migrate steadily from the trough to the outer slope. The migration direction is generally at a low angle to the inclination of the slope. Therefore, there is no definite area where the oil and gas can converge, thereby resulting in an unclear distribution of oil and gas in this type of slope. The ups and downs of terrain are developed when the gentle slope is characterized by relatively strong terrain deformations. In this type of slope, the oil and

* Corresponding author.
E-mail address: 1154229102@qq.com (X. Gao).

https://doi.org/10.1016/j.marpetgeo.2022.105661
Received 18 January 2021; Received in revised form 12 March 2022; Accepted 19 March 2022
Available online 23 March 2022
0264-8172/© 2022 Elsevier Ltd. All rights reserved.

gas will gradually converge at the local structural high points of the slope, causing the enrichment of oil and gas in these areas. Such structural high points commonly include nose-like structures and slope-break belts (containing syndepositional and structural slope-break belts). Weak tectonic slopes are characterized by extremely slow formational deformations and stable structural morphologies. Therefore, the oil and gas migration directions are roughly parallel to the inclination of the slope and have little changes in the migration process. Moreover, the slope gradients also influence the migration of oil and gas in the slope. Generally, the larger the slope gradient, the greater will be the migration force, which will be more conducive to the migration and accumulation of oil and gas in the slope. Overall, the slope is a favorable and important area of the sag for migration and accumulation of oil and gas (Rong et al., 2001; Li et al., 2003; Qiu et al., 2006; Yang et al., 2008; Zhao et al., 2012). Furthermore, gentle slopes are characterized by a large exploration area, accounting for one-third to half of the total area of the fault–sag. Practical explorations have shown that slopes have considerable quantities of hydrocarbon resources and great exploitation potential (Ren, 2009; Zhao et al., 2012). For example, medium–large oil fields in the southern slope of the Dongying Sag, the western slope of the Western Sag of the Liaohe Depression, and the western slope of the Biyang Sag are characterized by vast expanses of oil and gas reserves (Xiong, 2009; Gu, 2013; Jiang et al., 2016, Fig. 1a).

Zou et al. (2014) were the first to conduct research on the tectonic divisions of the Raoyang Sag based on some parameters, including the bottom curvature (Fig. 1a and b), density of faults, denudation rate, and derivatives of the strata thickness rate. They pointed out that the Lixian Slope was characterized by weak tectonic activities. As the name suggests, this weak tectonic slope is a special type of gentle slope that has been subjected to relatively weak tectonic activities during its whole developmental history (Zou et al., 2014; Zhao et al., 2014). Overall, the weak tectonic slopes are characterized by extremely slow formational changes, exceedingly low deformation degrees of the strata, stable structural morphologies and relatively underdeveloped faults (Zou et al., 2014; Zhao et al., 2014). Weak tectonic slopes usually form gentle terrains during their development (Gao et al., 2014). These slopes owe their unique characteristics of sequence stratigraphy, sedimentology and hydrocarbon accumulation to their distinct geological settings. Extensive research has been conducted, focusing on the tectonics, sequence stratigraphy, sedimentology, formational conditions, and mechanisms of oil and gas reservoirs of gentle slopes (Donaldson, 1974; Horne et al., 1976; Li, 2001, 2010; He, 2010; Mao, 2012; Gu, 2013; He et al., 2017a, 2017c; Zhu et al., 2017; Zhang et al., 2018). However, only a few studies were conducted under the concept of weak tectonic slopes (Zou et al., 2014; Zhao et al., 2014; Gao et al., 2014). Thus, there are considerable gaps in the knowledge regarding the characteristics, controls, and geological models of hydrocarbon accumulation in weak tectonic slopes. This significantly hinders the oilfield workers from achieving progress and breakthroughs in oil and gas exploration in such slopes.

This study has three objectives: 1) to discuss the characteristics and controls of hydrocarbon accumulation in the weak tectonic Lixian Slope; 2) to establish geological models for hydrocarbon accumulation in the Lixian Slope; and 3) provide recommendations for future explorations in the slope. This study is essential for guiding explorations on such slopes worldwide as well as enriching the theory of oil and gas accumulation and exploration in slopes to some extent.

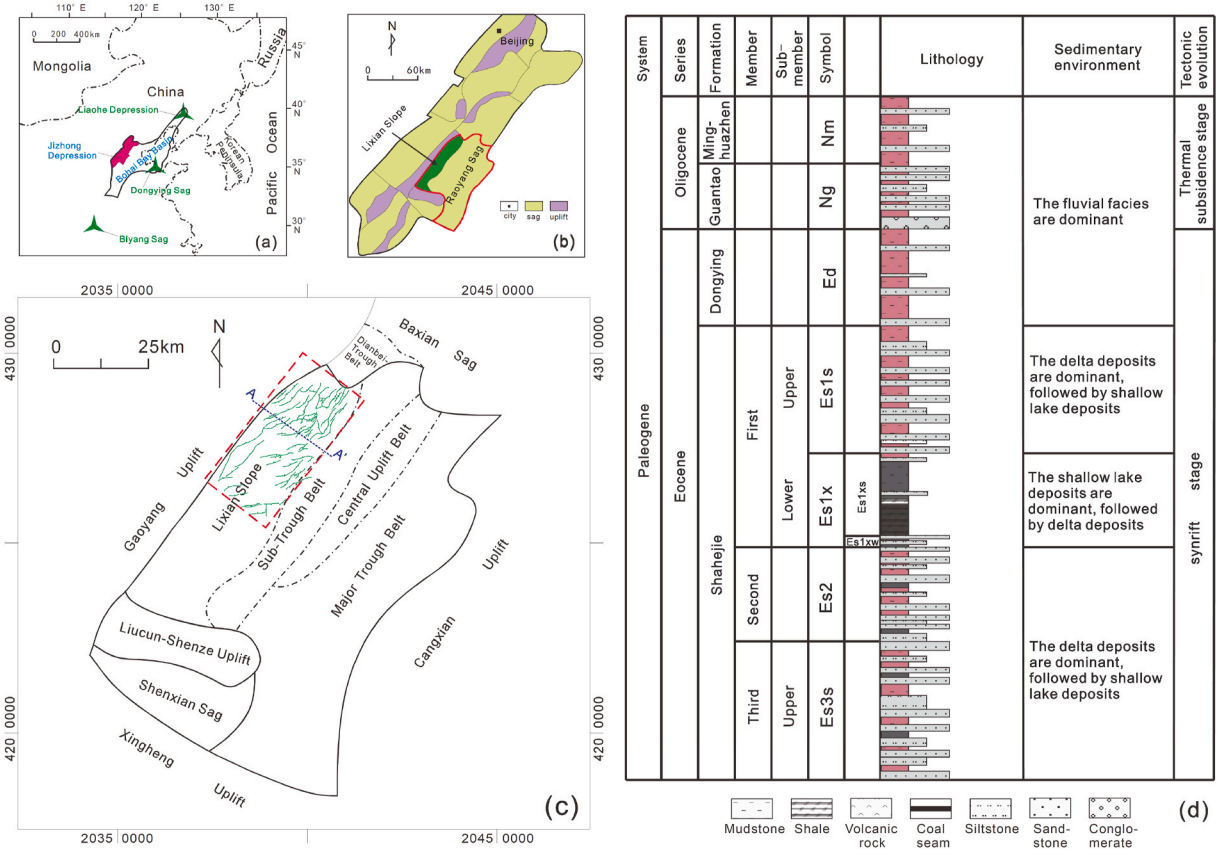

Fig. 1. (a) Locations of Bohai Bay Basin and Jizhong Depression. (b) Location of Raoyang Sag. (c) Tectonic belt division of Raoyang Sag, location of Lixian Slope, location of study area in this paper, and location of the seismic profile of Fig. 2. (d) Stratigraphic division, lithology, sedimentary environment and tectonic evolution of Lixian Slope, Raoyang Sag.

2. Geological background

The Raoyang Sag is one of the fault–sags in the Jizhong Depression, developed in the Bohai Bay Basin of Northern China (Fig. 1a and b). The Lixian Slope is located in the western part of the Raoyang Sag and acts as a secondary structural belt (Fig. 1c). The Raoyang Sag is broadly categorized into four tectonic belts, based on the structural positions and subsidence histories: Major Trough, Central Uplift, Sub–trough, and Lixian Slope (Fig. 1c). Among the slopes of the Jizhong Depression, the Lixian Slope occupies the maximum area, spanning approximately 2000 km^2, with a length and width of 90 and 20 km, respectively. Oil and gas exploration achievements have hardly been conducted in the south of the Lixian Slope, causing this area to be neglected by the Huabei Oilfield Company, which has the right to exploit this slope. Only a few wells have been drilled in the southern Lixian Slope, and the three-dimensional (3D) seismic data for this area has not been acquired yet. Taking these points under consideration, this study focuses on the Central–Northern Lixian Slope (Fig. 1c).

The tectonic evolution of the Bohai Bay Basin can be roughly divided into three chronological stages: (1) the first syn-rift stage during the Jurassic and Cretaceous; (2) the second syn-rift stage during the Paleogene; and (3) a thermal subsidence stage during the Neogene and Quaternary (Yang and Xu, 2004; Qi and Yang, 2010). During the Early Paleozoic, an epeiric sea dominated the North China Plate in which the Bohai Bay Basin is located. Eventually, in the Late Paleozoic, the North China Plate collided with the Siberian Plate to the north and the Yangtze Plate to the south, thus suturing the three in the Early Mesozoic (Ren, 1994). The alternation of depositional environments between marine and continental prevailed during the Late Paleozoic (Zhu, 2009). This was followed by the subduction of the Pacific Plate, situated to the east of the then sutured plate during the Early Mesozoic, resulting in the formation of the Bohai Bay Basin (Zhu, 2009; Qi and Yang, 2010). The Late Cretaceous witnessed the weakening of the Pacific Plate subduction process, causing the extrusion and consequent rise of the Bohai Bay Basin (Chen, 2019). At this syn-rift stage, the deposition was dominated by lacustrine and alluvial deposits intercalated with volcanic rocks and coal seams (Xiao, 2007). Later, in the Early Paleogene, the Pacific Plate was again subducted under the sutured plate, causing further development of the Bohai Bay Basin under a strongly extensional regime (Zhao, 1984; Chen, 2019). As a result, many depressions and numerous sags, including the Raoyang Sag, were developed in the Bohai Bay Basin during the Paleogene. The deposition occurred widely across the basin during the Paleogene. Due to the change in the subduction direction, its impact on the Bohai Bay Basin weakened in the Late Paleogene (Miao, 2018). The Bohai Bay Basin then entered the thermal subsidence stage during the Neogene and Quaternary and was characterized by considerably weak tectonic activity and stable deposition (Yang and Xu, 2004; Qi and Yang, 2010; Chen, 2019).

A vast majority of the oil and gas reservoirs discovered in the Lixian Slope are located in the Paleogene strata (Ren, 2009; Zhao et al., 2012; Li, 2016). Hence, the Paleogene strata have been examined explicitly in this study. The Paleogene strata of the Raoyang Sag can be divided into the Eocene Kongdian Formation (Ek Formation), the Eocene Shahejie Formation (Es Formation), and the Oligocene Dongying Formation (Ed Formation) (Fig. 1d). In addition, the Es Formation contains three members, Es3, Es2, and Es1. Moreover, the Es3 and Es1 members can be further divided into two sub–members: the lower part (Es3x and Es1x sub–members) and the upper part (Es3s and Es1s sub–members) (Fig. 1d).

In the Early Paleogene, the deposition of Ek Formation and Es3x Sub–member occurred prominently in the eastern Raoyang Sag and was fairly absent in the Lixian Slope (Ren, 2009; He et al., 2017b, 2017c). Delta deposits dominated the Lixian Slope during the deposition of the Es3s Sub–member and Es2 Member, with lake deposits covering smaller areas along the eastern part of the slope (Ren, 2009). Thus, both the Es3s Sub–member and Es2 Member have similar lithologies and are mainly composed of fine-grained sandstones, siltstones, and mudstones (Fig. 1d). At the onset of the deposition of the Es1x Sub–member, relatively short-term delta deposits developed widely across the Lixian Slope (Ren, 2009). This was followed by an extensive lake transgressional event, which caused the predominance of lacustrine facies in the Lixian Slope during the deposition of the Es1x Sub–member (Ren, 2009). Thus, the Es1x Sub–member consists of a thin interval (Es1xw Interval) composed of fine-grained sandstones, siltstones, and mudstones as well as a much thicker interval (Es1xs Interval) composed of mudstones and oil shales intercalated with biolimestones, marls, and salt-gypsum rocks (Fig. 1d). The delta facies also dominated the Lixian Slope during the deposition of Es1s Sub–member (Ren, 2009), whereas the lacustrine facies occupied small areas on the eastern slope. This implies that the Es1s Sub–member of the Lixian Slope mainly consists of fine-grained sandstones, siltstones, and mudstones (Fig. 1d). The Ed Formation was deposited in a fluvial environment (Ren, 2009) and is composed of mudstones intercalated with siltstones and sandstones (Fig. 1d).

3. Data and methods

The gradients of the Lixian Slope during the deposition of Es3, Es2, and Es1 members were studied based on the 3D seismic data provided by the Exploration Research Institute of Huabei Oilfield. These gradients were examined by flattening the top surfaces of these members. The faults in the Lixian Slope were identified, and their distribution, tectonic history, and throw characteristics were assessed based on the 3D seismic data. Based on the logging data of approximately 100 wells, we completed the isopach map of the special lithologic interval, developed within the Es1x Sub–member and mainly composed of gray-black/black oil shales and mudstones, and the contour maps of the sandstone-to-strata ratios for the Es3 Member, Es2 Member, Es1xw Interval, Es1xs Interval, Es1s Sub–member, and Ed Formation. The special lithologic intervals act as source rocks. The sandstone-to-strata ratio is defined as the ratio of the total thickness of sandstones to that of the corresponding individual stratum (Fu et al., 2014). Data on the physical properties of crude oil for 151 oil samples and the physical properties of sandstone for 251 samples were provided by the Exploration Research Institute of Huabei Oilfield. These samples were chosen evenly from each Paleogene stratum. The physical properties of crude oil include the gravity, viscosity, and wax and sulfur contents, whereas the physical properties of sandstone include porosity and permeability values.

A total of 19 source rock samples and 27 crude oil samples were chosen for gas chromatography–mass spectrometry (GC–MS) analyses. Moreover, 13, 3, and 3 samples were selected from Es1x, Es3x, and Ek–Es4 source rocks, respectively. The saturated hydrocarbons obtained from the isolated extractable organic matter through liquid column chromatography were used for GC–MS analyses. The GC–MS analyses were conducted using an Agilent 6890N gas chromatograph and SSQ 7000 mass spectrometer, based on the procedures presented in He et al. (2017b).

4. Results

4.1. Slope gradients

The Lixian Slope developed since the onset of deposition of the Es3 Member and was subjected to weak tectonic activities during its development. During the deposition of the Es3 Member, the Lixian Slope had exceptionally low gradients, which ranged from 0.45° to 1.09°, while the area adjacent to the Sub–trough displayed a slightly higher gradient (Fig. 2a). During the deposition of the Es2 Member, the Lixian Slope was characterized by a lower gradient value, approximately 0.18° (Fig. 2b). The gradient of the slope increased slightly and was approximately 0.54° during the deposition of the Es1 Member (Fig. 2c). Raoyang Sag entered an uplift stage and was gradually filled during the deposition of the Ed Formation (Ren, 2009). The Bohai Bay Basin then entered a thermal

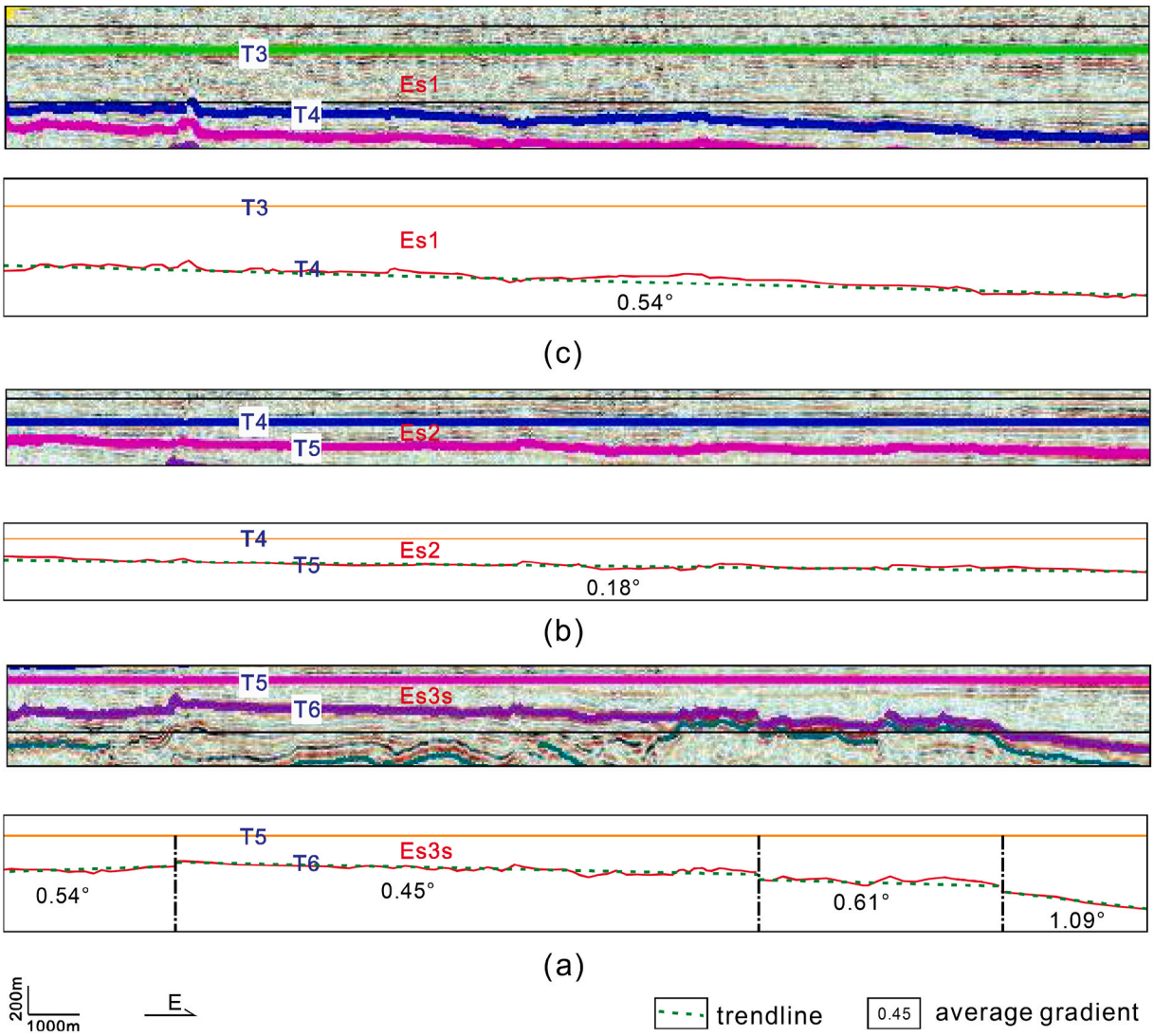

Fig. 2. Seismic profile shows the gradients of Lixian Slope during the deposition of Es1 Member (a), Es2 Member (b) and Es3 Member (c). The location of this Seismic profile is marked in Fig. 1c and named AA'.

subsidence stage during the Neogene and the Quaternary (Chen, 2019). Thus, the slope almost maintained a flat terrain after the deposition of the Es Formation. Overall, the Lixian Slope had shallow gradients throughout its development.

4.2. Fault characteristics

The faults in Lixian Slope are underdeveloped, and those in the north of the slope are developed better than those in the south (Fig. 3a). Almost all faults in the Lixian Slope are normal faults, trending NNE–NEE and N–W. In addition, NNE–NEE trending faults are significantly dominant. The development of NNE–NEE trending faults, except few such as the Gaoyang Fault (Mj1) and Dabaichi Fault (Mj2) that began to be developed in the Early Paleogene, mainly began along with the deposition of the Es2 and Es1 members (Fig. 3a). A part of the NNE–NEE trending faults gradually reached a hiatus toward the end of deposition of the Ed Formation. In contrast, others stopped developing during the deposition of the Guantao to Minghuazhen Formations. The N–W trending faults generally began to form before the Paleogene. The process stopped at the end of the sedimentation of the Es3 Member. Compared to the N–W trending faults, the NNE–NEE faults formed much later and were characterized by longer durations of tectonic activities.

Most of the faults exhibit extremely low throws (<30 m) during their entire developmental stages. Fig. 3b illustrates the fault throws of major faults in the Lixian Slope during the deposition of the Es3, Es2, and Es1 members and the Ed Formation. The results show that, during the deposition of the Es3 Member, only the Gaoyang (Mj1), Dabaichi (Mj2), Mj6, and Mj4 Faults had significant fault throws of approximately 240, 100, 50, and 20 m, respectively (Fig. 3b). The development of rest of the major faults did not begin during this period. During the deposition of the Es2 Member, most of these major faults had considerably low fault throws (<5 m), except the Gaoyang Fault (Mj1) and Mj4 Fault that had relatively high fault throws of approximately 30 and 20 m, respectively (Fig. 3b). During the deposition of the Es1 Member, both the Mj9 and Mj10 Faults, developed in the north of the slope and adjacent to the Sub–trough, exhibiting substantially higher fault throws of approximately 150 m. The Mj3, Mj7, and Mj8 Faults had similar fault throws ranging from 40 to 60 m, whereas the remaining significant faults had considerably lower throws (<20 m) (Fig. 3b). In addition, numerous antithetic faults are developed well in the Lixian Slope. An antithetic fault is a fault whose inclination is generally opposite to that of the slope.

4.3. Characteristics and classification of crude oils

Based on the biomarker distributions of the saturated hydrocarbons, three different groups of oils have been recognized in the Lixian Slope.

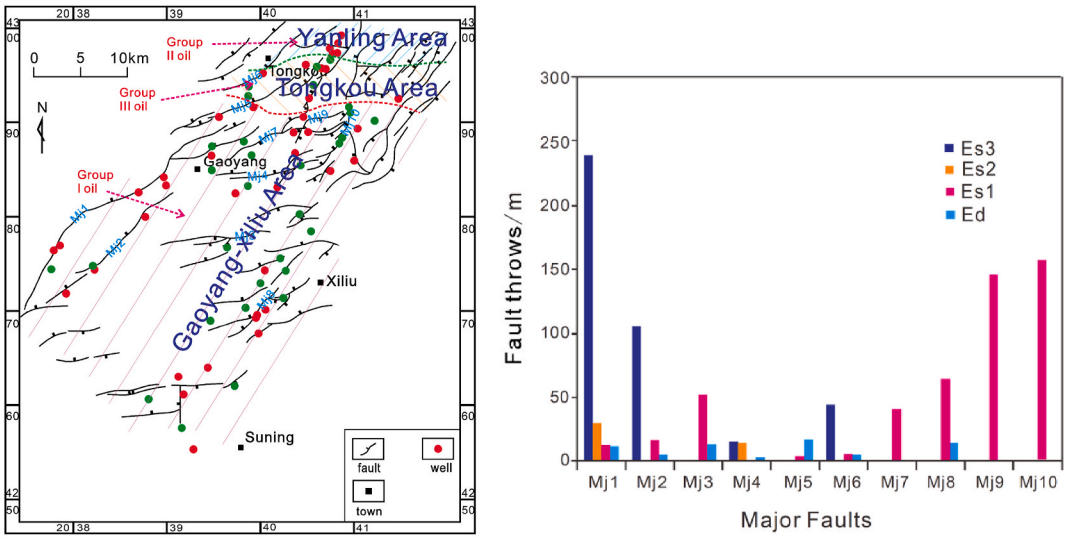

Fig. 3. (a) Overlayed map shows the plane distribution of faults in Lixian Slope, and the plane distributions of commercial oil-wells (red), low producing oil-wells (green), faults and planar distributions of Group I, II, and III oils in Paleogene, in Lixian Slope. (b) The fault throws of major faults in Lixian Slope during the deposition of Es1 Member, Es2 Member and Es3 Member, respectively. (For interpretation of the references to colour in this figure legend, the reader is referred to the Web version of this article.)

Group I oils are distributed in most areas of the Lixian Slope, mainly in the Gaoyang and Xiliu areas (Fig. 12). Group II and group III oils are distributed in much smaller areas and are found in the Yanling and Tongkou areas, respectively (Fig. 12). The Yanling area is located in the northernmost part of the study area. Tongkou area is adjacent to the Yanling area in its north; it is located between the Gaoyang and Yanling areas (Fig. 12). N-alkanes of oil samples from different groups are distributed widely and usually vary from *n-C*$_{14}$ to *n-C*$_{35}$. The pristane to *n-C*$_{17}$ alkane (*Pr/n-C17*), phytane to *n-C*$_{18}$ alkane (*Ph/n-C18*), and pristine to phytane (Pr/Ph) ratios are usually used to estimate

Table 1
Parameters of n-alkanes, isoprenoid, terpane and sterane of the crude oils of Paleogene, Lixian Slope.

Area	Well name	Depth	Member	*Pr/Ph*	*Pr/n-C*$_{17}$	*Ph/n-C*$_{18}$	*Ga/C*$_{31}$*H*	Ts/(Tm + Ts)	C$_{32}$–S/(S + R)	C$_{29}$-20S (%)	C$_{29}$-ββ/(%)	%C$_{27}$	%C$_{28}$	%C$_{29}$
Gaoyang–Xiliu area	G34	2588	Es1	0.19	1.33	7.12	1.89	0.18	0.53	0.24	0.21	42.3	19.44	38.26
	G36	2776	Es1	0.16	1.45	10.45	3.23	0.15	0.52	0.23	0.20	37.45	19.83	42.72
	G58	2596	Es1	0.18	1.35	12.47	3.42	0.14	0.36	0.11	0.18	32.62	21.13	46.25
	G64	2328.9	Es1	0.19	1.29	8.41	3.04	0.25	0.46	0.20	0.19	36.18	20.67	43.15
	G17	2692	Es1	0.30	1.61	5.94	2.05	0.37	0.44	0.25	0.19	34.13	24.55	41.32
	G18	2654	Es1	0.23	1.39	6.93	2.30	0.39	0.47	0.33	0.24	31.54	26.38	42.09
	G28	2353.1	Es2	0.25	1.1	3.94	1.49	0.17	0.51	0.29	0.19	38.75	21.56	39.69
	G30	2541.9	Es2	0.31	1.45	5.73	2.45	0.35	0.40	0.26	0.18	31.67	23.81	44.51
	D32	3040	Es3	0.19	1.34	7.53	1.85	0.14	0.49	0.28	0.27	39.81	19.07	41.12
	G43	3097	Es3	0.32	1.32	5.51	2.00	0.16	0.51	0.31	0.19	46.15	21.68	32.17
	XL7	3281.3	Es1	0.21	1.40	6.20	1.83	0.31	0.53	0.31	0.22	38	19	43
	XL101	3288.8	Es1	0.23	1.21	5.14	2.00	0.40	0.48	0.19	0.19	35.9	23.9	40.2
	XL102	3331.6	Es1	0.24	1.39	5.04	2.35	0.47	0.46	0.22	0.19	38.92	20.99	40.09
	XL9	3188.5	Es2	0.24	1.26	5.11	1.99	0.15	0.52	0.24	0.18	37	19.36	43.64
	XL9	3200.8	Es2	0.25	1.23	5.45	1.58	0.17	0.53	0.29	0.20	35.28	22.1	42.62
	XL109	3144	Es2	0.38	1.52	5.71	2.02	0.43	0.49	0.20	0.19	39	19.59	41.41
	XL9	3335.5	Es3	0.28	1.04	3.91	1.49	0.18	0.51	0.32	0.19	36.01	20.69	43.3
Yanling area	G59	2602.96	Es1	0.66	0.48	0.79	0.66	0.53	0.59	0.28	0.21	32.47	21.97	45.56
	G60	2618	Es1	0.74	0.57	0.79	0.58	0.49	0.56	0.26	0.23	36.13	20.2	43.67
	Y50-1	2588	Es1	0.67	0.47	0.68	0.49	0.51	0.60	0.24	0.22	31.4	19.3	49.3
	Y107	2812	Es2	0.62	0.48	0.77	0.54	0.55	0.59	0.29	0.26	35.1	21.3	43.6
	D15	3128.8	Es2	0.81	0.42	0.52	0.39	0.54	0.58	0.27	0.24	33.2	20.8	46
	Y60-3	2695	Es3	0.67	0.46	0.69	0.48	0.52	0.59	0.24	0.23	35.1	21.3	43.6
Tongkou area	Y60-2	2683.3	Es2	0.36	0.62	1.84	0.99	0.43	0.59	0.23	0.19	34.8	19.9	45.3
	Y63-4	2643.2	Es2	0.34	0.61	1.87	/	/	/	/	/	/	/	/
	Y68	2741.9	Es2	/	/	/	0.95	0.44	0.50	0.22	0.18	24.71	15.4	59.89
	Y22	2910.1	Es3	0.30	0.68	2.31	1.14	0.40	0.60	0.31	0.22	33.91	19.51	46.58

Pr/Ph = Pristane/Phytane; Pr/C17 = Pristane/C17 n-alkane; Ph/C18 = Phytane/C18 n-alkane; Ga/C$_{31}$H = Gammacerane/C31 homohopane; Ts/(Tm + Ts) = C27 18a(H)-22, 29, 30-trisnorneohopane/[C27 17a(H)-22, 29, 30-trisnorhopanen + C27 18a(H)-22, 29, 30trisnorneohopane]; C32–S/(S + R) = C32 homohopane 22S/(C32 homohopane 22S + C32 homohopane 22R); C29–20S(%) = C29 sterane ααα 20S/(20S + 20R); C29-ββ/(%) = C29 sterane αββ/(αββ+ααα); %C27 = C27 steranes/(C27 steranes + C28 steranes + C29 steranes); %C28 = C28 steranes/(C27 steranes + C28 steranes + C29 steranes); %C29 = C29 steranes/(C27 steranes + C28 steranes + C29 steranes); "/" = No data.

paleoenvironmental conditions of source rocks (Peters and Moldowan, 1993; Hanson et al., 2000). Group I oil samples have high *Pr/n-C17* values (1.04–1.61, average = 1.33), high *Ph/n-C18* values (3.91–12.47, average = 6.51), but low *Pr/Ph* values (0.16–0.38, average = 0.24) (Table 1; Fig. 4a and b). Group II oil samples show much lower *Pr/n-C17* (0.42–0.57, average = 0.48) and *Ph/n-C18* values (0.52–0.79, average = 0.71), but higher *Pr/Ph* values (0.62–0.81, average = 0.70) (Table 1; Fig. 4a and b). The *Pr/n-C17*, *Ph/n-C18*, and *Pr/Ph* values of group III oils are between those of group I and group II oils, and range from 0.61 to 0.68, 1.84 to 2.31, and 0.30 to 0.36 with average values of 0.64, 2.01, and 0.33, respectively (Table 1; Fig. 4a and b).

Proportional sterane abundances are useful for indicating organic matter sources (Seifert and Moldowan, 1978). The group I, II, and III oils have similar relative abundances of regular steranes C_{27}, C_{28}, and C_{29}. The average relative abundances of regular steranes C_{27}, C_{28}, and C_{29} are 37.1%, 21.4%, and 41.5% in group I oils, 33.9%, 20.8%, and 45.3% in group II oils, and are 31.1%, 18.3%, and 50.6% in group III oils, respectively (Table 1). Gammacerane is a specific biomarker for stratified water column, often associated with salinity stratification (Fu et al., 1986; Chen et al., 2014). Group I oil samples are characterized by much higher gammacerane/C_{31} homohopane values, varying from 1.49 to 3.42 with an average of 2.18 (Table 1; Fig. 4b). The group II oil samples have much lower gammacerane/C_{31} homohopane values, ranging from 0.39 to 0.66 with an average of 0.52 (Table 1; Fig. 4b). The gammacerane/C_{31} homohopane values of group III oils are also between group I and II oils and range from 0.95 to 1.14, with an average of 1.03 (Table 1; Fig. 4b). The *Ts/(Tm + Ts)*, C_{32} homohopane $S/(S+R)$, C_{29} sterane ααα 20S/(20S + 20R), and C_{29} sterane αββ/(αββ + ααα) are usually regarded as thermal maturity parameters. Table 1 lists the *Ts/(Tm + Ts)*, C_{32} homohopane $S/(S+R)$, C_{29} sterane ααα 20S/(20S + 20R), and C_{29} sterane αββ/(αββ + ααα) values of group I, II, and III oil samples. Fig. 4c shows that the group II oil samples have high maturity, the group I oil samples have low maturity, and the maturity of group III oil samples are almost between them. However, Fig. 4d displays no significant differences among them, and the maturity of group II oil samples is slightly higher than that of the group I and group III oil samples.

The physical properties of crude oil are important for obtaining further information on the source rock maturity trend and hydrocarbon migration direction (He and Xia, 2017). Generally, the scale of crude oil physical property data is much larger than that of the geochemical data. The crude oils in the Gaoyang area have high gravity values (average = 0.9144 g/cm^3), high viscosity values (average = 677.71 mPa s), low wax contents (average = 10.89%), but high sulfur contents (average = 0.78%) (Table 2; Fig. 5). The gravity and viscosity values of crude oils in

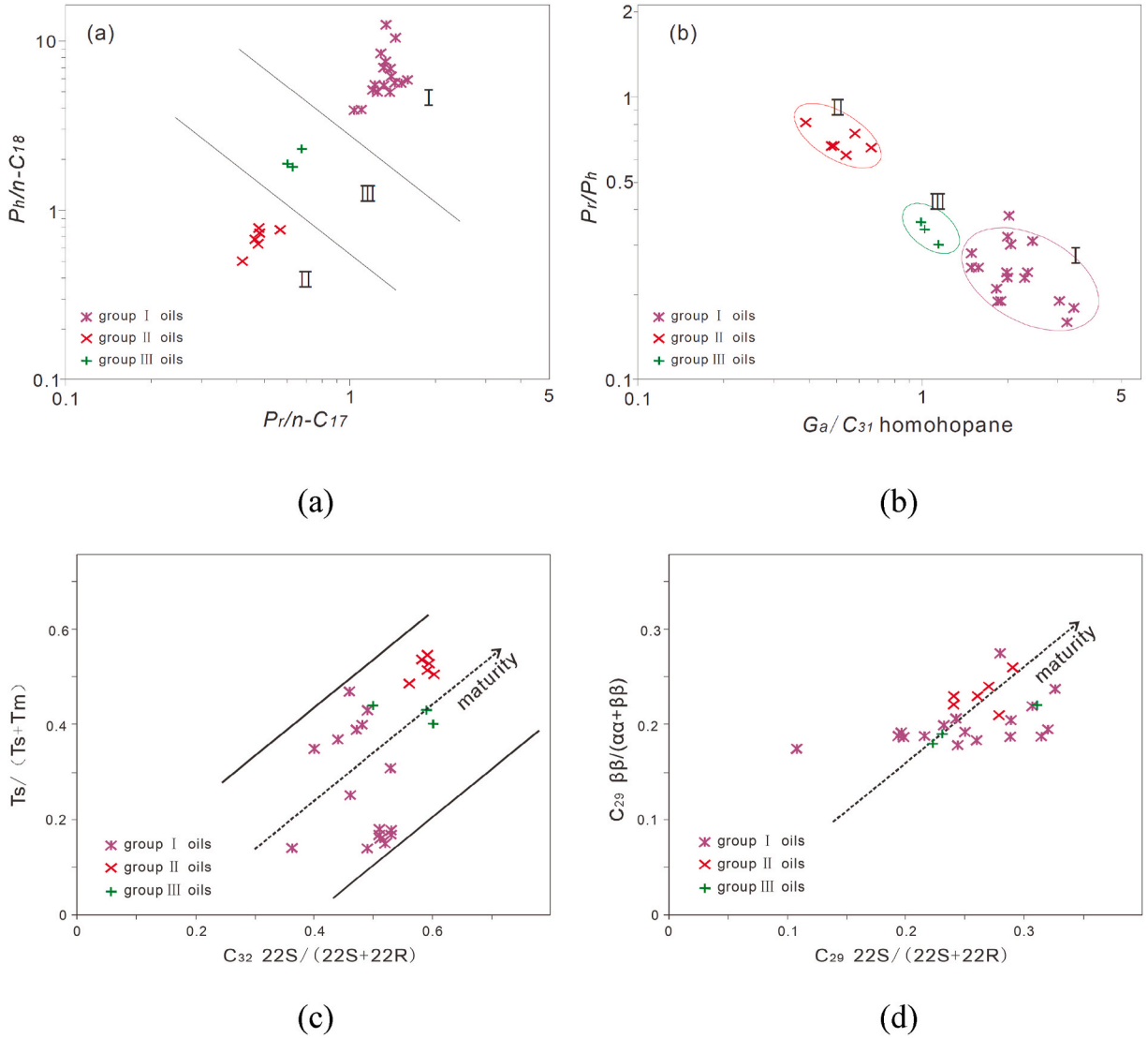

Fig. 4. (a) Cross plot of *Pr/n-C17* versus *Ph/n-C18*, (b) of *Pr/Ph* versus *Ga (gammacerane)/C31 homohopane* of crude oils in Paleogene, (C) of *Ts/(Tm + Ts)* versus *C32 homohopane S/(S + R)* and (d) of *C29 sterane ααα 20S/(20S + 20R)* versus *C29 sterane αββ/(αββ+ααα)* of crude oils in Paleogene, Lixian Slope.

Table 2
Bulk physical properties of crude oils in Paleogene, Lixian Slope.

Area	Gravity (g/cm^3)	Viscosity (mPa.s)	Wax contents (%)	Sulfur contents (%)
Gaoyang area	0.8857–0.9312 (0.9144)	38.62–2273.30 (677.71)	5.75–17.68 (10.89)	0.27–1.50 (0.78)
Xiliu area	0.8871–0.9709 (0.9139)	62.9–4416.0 (538.07)	4.80–21.90 (13.15)	0.22–0.95 (0.59)
Yanling area	0.8549–0.9053 (0.8740)	9.21–52.99 (24.11)	11.60–20.61 (16.77)	0.05–0.45 (0.28)
Tongkou area	0.8586–0.9171 (0.8913)	10.83–359.39 (108.38)	9.5–19.84 (16.24)	0.06–0.68 (0.41)

Note: maximum value-minimum value (average value).

the Xiliu area have a relatively wide range, with average values of 0.9139 g/cm^3 and 538.07 mPa s, respectively (Table 2; Fig. 5). The wax and sulfur contents of the crude oils in the Xiliu area are similar to those in the Gaoyang area. The crude oils in the Xiliu area have low wax contents (average = 13.15%) and high sulfur contents (average = 0.59%) (Table 2; Fig. 5). However, the crude oils in the Yanling area are characterized by much lower gravity than those in the Gaoyang and Xiliu areas (average = 0.8740 g/cm^3) and viscosity values (average = 24.11 mPa s) (Table 2; Fig. 5), low sulfur contents (average = 0.28%), and high wax contents (average = 16.77%) (Table 2). Fig. 5 shows that most of the crude oils in the Tongkou area fall into the intermediate zone. The gravity and viscosity values of these oils vary from 0.8586 g/cm^3 to 0.9171 g/cm^3 (average = 0.8913 g/cm^3) and from 10.83 mPa s to 359.39 mPa s (average = 108.38 mPa s), respectively (Table 2). Moreover, the average wax and sulfur contents of the crude oils in the Tongkou area are 16.24% and 0.41%, respectively (Table 2).

4.4. Characteristics of source rocks

There are three sets of source rocks in the Lixian Slope and its adjacent area. The Es1x source rocks are actually a special lithologic interval that consists of gray-black/black oil shales and mudstones intercalated with marls, salt-gypsum rocks, and biolimestones. The Es1x source rocks have been evaluated as fair to excellent source rocks, dominated by type II1 kerogens, and the average total organic carbon content of Es1x source rocks is 1.68% (Zhao et al., 2012, Table 3). The Es1x source rocks are developed well in the slope and distributed almost across the entire slope, except for a small zone in the southwest of study area (Fig. 6). The thickness of the Es1x source rocks in the slope mainly ranges from 0 to 160 m, with an average of approximately 60 m. At present, the Es1x source rocks are generally in the hydrocarbon expulsion stage, while they are mostly of low maturities (Zhao et al., 2012, Table 3). The Es3x Sub–member has been evaluated as a set of fair source rocks with an average of 1.05% (Table 3). The organic matters of Es3x source rocks are dominated by type II2 and are generally mature (Table 3). The Es3x source rocks are mainly developed in the troughs of the Raoyang Sag, meaning that they are commonly located to the east of the Lixian Slope (Fig. 6). These source rocks are composed of dark mudstones mixed with black shales and have relatively large thicknesses with an average of more than 200 m (Fig. 6). Most of the Es3x source rocks have large burial depths, indicating that they are located in mature stages (Zhao et al., 2012). Previous studies have pointed out that the mature Ek–Es4 source rocks are mainly developed in the area located to the north of the Tongkou area (Ren, 2009; Zhao et al., 2012) (Fig. 6). The organic matters of Es3x source rocks are generally mature and mainly composed of type II2 (Table 3).

Table 4 lists the biomarkers of n-alkanes, isoprenoids, terpanes and steranes of the tested samples from Es1x, Es3x and Ek-Es4 source rocks. The n-alkanes of the Es1x source rocks are distributed widely and vary from $n\text{-}C_{14}$ to $n\text{-}C_{35}$. The Es1x source rocks have high $Pr/n\text{-}C_{17}$ values in the range of 0.77–1.64 (average = 1.22), high $Ph/n\text{-}C_{18}$ values in the range of 3.10–8.60 (average = 5.80), and low Pr/Ph values in the range of 0.11–0.39 (average = 0.24), indicating an obvious dominance of phytane (Table 4). Furthermore, the Es1x source rocks are characterized by high gammacerane/C_{31} homohopane values ranging from 1.31 to 4.79 (average = 2.37) (Table 4). The distribution characteristics of n-alkanes in the Es3x and Ek–Es4 source rock samples are similar to those in the Es1x source rock samples. In the Es3x and Ek–Es4 source rock samples, the n-alkanes have wide distributions, usually varying from n-

Table 3
Lithology, average TOC, organic matter type and organic matter maturity of Es1x, Es3x and Ek-Es4 source rocks of Paleogene, Lixian Slope.

Source rock	Lithology	Average TOC (%)	Type	Maturity
Es1x	Oil shale/ Mudstone	1.68	II1	Immature-low maturity
Es3x	Mudstone	1.05	II2	mature
Ek-Es4	Mudstone	0.83	II2	mature

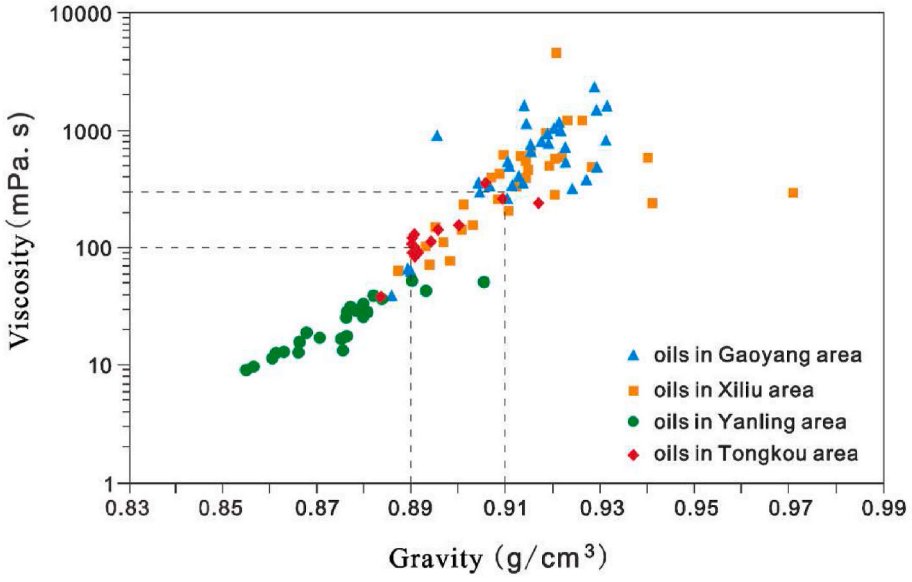

Fig. 5. Cross plot of density versus viscosity of crude oils in Paleogene, Lixian Slope.

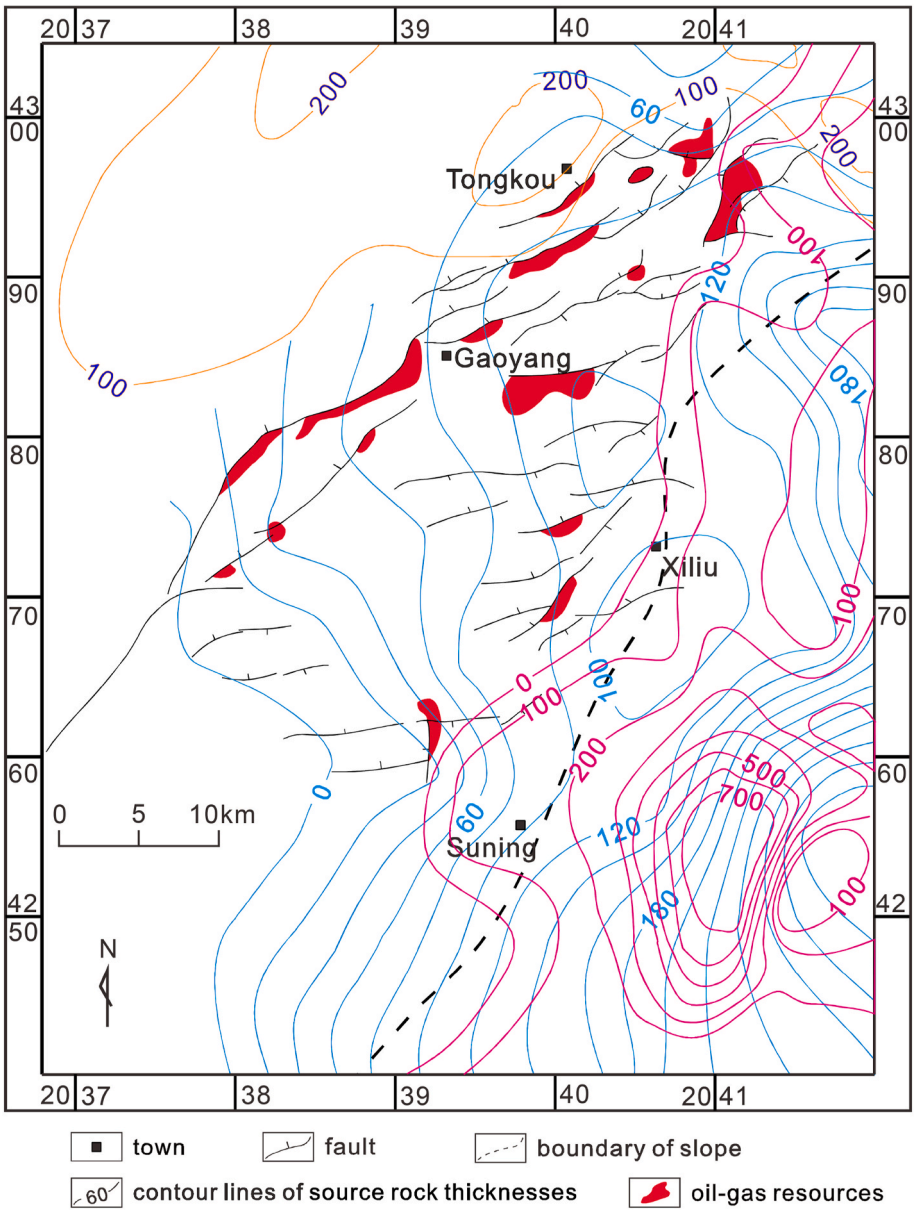

Fig. 6. (a). Overlayed map shows the plane distribution of Es1x (blue contour lines), Es3x (red contour lines), Ek-Es4 (orange contour lines) source rocks in Lixian Slope and neighboring region, and the plane distribution of oil-gas reservoirs. (For interpretation of the references to colour in this figure legend, the reader is referred to the Web version of this article.)

C_{14} to n-C_{35}. Compared to the Ek–Es4 source rock samples, the Es3x have higher Pr/n-C_{17}, Ph/n-C_{18}, and gammacerane/C_{31} homohopane values but lower Pr/Ph values. The average Pr/n-C_{17}, Ph/n-C_{18}, gammacerane/C_{31} homohopane, and Pr/Ph values of Es3x source rocks are listed in Table 4. In addition, all samples from different source rocks have similar relative abundances of regular steranes C_{27}, C_{28}, and C_{29}. The average relative abundances of regular steranes C_{27}, C_{28}, and C_{29} in Es1x source rocks are 36.8%, 20.7%, and 42.5%, those in the Es3x source rocks are 33.6%, 22.5%, and 43.9%, and those in the Ek–Es4 source rocks are 39.4%, 15.9%, and 44.7%, respectively (Table 4).

4.5. Characteristics of sandstones

4.5.1. Physical properties of sandstones

According to previous research on sedimentary facies and their distribution in the Lixian Slope, it can be inferred that the reservoir rocks of the Paleogene are dominated by sandstones, with minor amounts of carbonate rocks, which were developed in the Es1x Sub–member (Ren, 2009). This study focuses on the sandstones. The Paleogene sandbody strata consist of delta sandstones and fluvial sandstones along with a few shore-shallow lacustrine beach bar sandstones.

The physical properties of Es3, Es2, and Es1 sandstones are similar to each other. The average porosity and permeability value of sandstones in each member of the Es Formation is approximately 15%–18% and 70 $\times 10^{-3}$ μm^2–80 $\times 10^{-3}$ μm^2, respectively (Fig. 7a, b, c). Around 60% of the Es3 sandstone samples, 80% of the Es2 sandstone samples, and 70% of the Es1 sandstone samples have relatively high porosity values greater than 15% (Fig. 7a, b, c). The samples with a high permeability value greater than 10 $\times 10^{-3}$ μm^2 account for 70% of Es3 sandstone samples, 80% of Es2 sandstone samples, and 70% of Es1 sandstone samples (Fig. 7a, b, c). Therefore, Es sandstones have been mainly evaluated as medium porosity and medium permeability reservoir rocks. The average porosity and permeability values of the Ed sandstones are approximately 19.0% and 440 $\times 10^{-3}$ μm^2, respectively (Fig. 7d). The samples with a

Table 4
Parameters of n-alkanes, isoprenoid, terpane and sterane of Es1x source rocks of Paleogene, Lixian Slope.

Well name	Depth	Member	*Pr/Ph*	*Pr/n-C*$_{17}$	*Ph/n-C*$_{18}$	*Ga/C*$_{31}$*H*	*Ts/(Tm + Ts)*	C$_{32}$–*S/(S + R)*	C$_{29}$-20*S* (%)	C$_{29}$-*ββ*/(%)	%C$_{27}$	%C$_{28}$	%C$_{29}$
G24	2625.8	Es1x	1.53	7.96	0.21	1.92	0.41	0.39	0.20	0.22	30.7	19.5	49.8
G34	2511.4	Es1x	0.77	4.07	0.21	2.79	0.23	0.52	0.11	0.25	33.7	23.1	43.2
G38	2642	Es1x	1.35	4.56	0.35	1.82	0.24	0.42	0.15	0.16	35.4	17.9	46.7
G46	2800	Es1x	1.07	3.10	0.39	2.23	0.27	0.42	0.14	0.17	39.4	18.7	41.9
G52	3094.2	Es1x	1.60	8.60	0.14	4.79	0.15	0.48	0.17	0.22	42.6	20.1	37.3
G52	3094.4	Es1x	1.64	7.76	0.20	2.39	0.35	0.56	0.17	0.21	41.2	16.2	42.6
G58	2596	Es1x	0.94	6.98	0.18	3.42	0.23	0.45	0.12	0.23	33.9	26.7	39.4
G59	2610	Es1x	1.05	5.68	0.25	2.27	0.29	0.44	0.12	0.20	39.0	21.1	39.9
XL11	3418.5	Es1x	1.22	5.99	0.15	1.80	0.18	0.50	0.25	0.22	41.7	16.3	42.0
XL5	3370.2	Es1x	1.24	5.52	0.22	1.31	0.24	0.44	0.20	0.24	39.1	21.6	39.3
XL5	3372.2	Es1x	1.23	7.17	0.12	2.06	0.23	0.56	0.17	0.19	30.9	22.1	47.0
XL5	3375.7	Es1x	1.17	7.38	0.11	1.67	0.25	0.43	0.19	0.18	34.4	16.2	49.4
XL5	3378.6	Es1x	1.10	4.54	0.16	2.28	0.20	0.43	0.19	0.20	45.0	23.0	32.0
L489	3586.1	Es3x	1.23	1.86	0.61	0.99	0.39	0.54	0.33	0.21	28.8	27.0	44.2
N45	3629.2	Es3x	0.71	1.45	0.42	0.86	0.27	0.55	0.25	0.21	43.8	18.4	37.8
Y24	3133.4	Es3x	0.67	1.40	0.42	0.76	0.49	0.57	0.36	0.34	28.3	22.27	49.5
XinL1	4472.5	Es4-Ek	/	/	/	/	0.58	0.63	0.44	0.38	43.1	17.8	39.1
XinL1	5080	Es4-Ek	0.51	0.56	0.92	0.50	0.36	0.52	/	/	/	/	/
Y118	2725.2	Es4-Ek	0.50	1.00	0.56	0.51	0.05	0.62	0.30	0.18	36.58	10.23	53.19

Pr/Ph = Pristane/Phytane; Pr/C17 = Pristane/C17 n-alkane; Ph/C18 = Phytane/C18 n-alkane; Ga/C$_{31}$H = Gammacerane/C31 homohopane; Ts/(Tm + Ts) = C27 18a(H)-22, 29, 30-trisnorneohopane/[C27 17a(H)-22, 29, 30-trisnorhopanen + C27 18a(H)-22, 29, 30trisnorneohopane]; C32–S/(S + R) = C32 homohopane 22S/(C32 homohopane 22S + C32 homohopane 22R); C29–20S(%) = C29 sterane ααα 20S/(20S + 20R); C29-ββ/(%) = C29 sterane αββ/(αββ+ααα); %C27 = C27 steranes/(C27 steranes + C28 steranes + C29 steranes); %C28 = C28 steranes/(C27 steranes + C28 steranes + C29 steranes); %C29 = C29 steranes/(C27 steranes + C28 steranes + C29 steranes); "/" = No data.

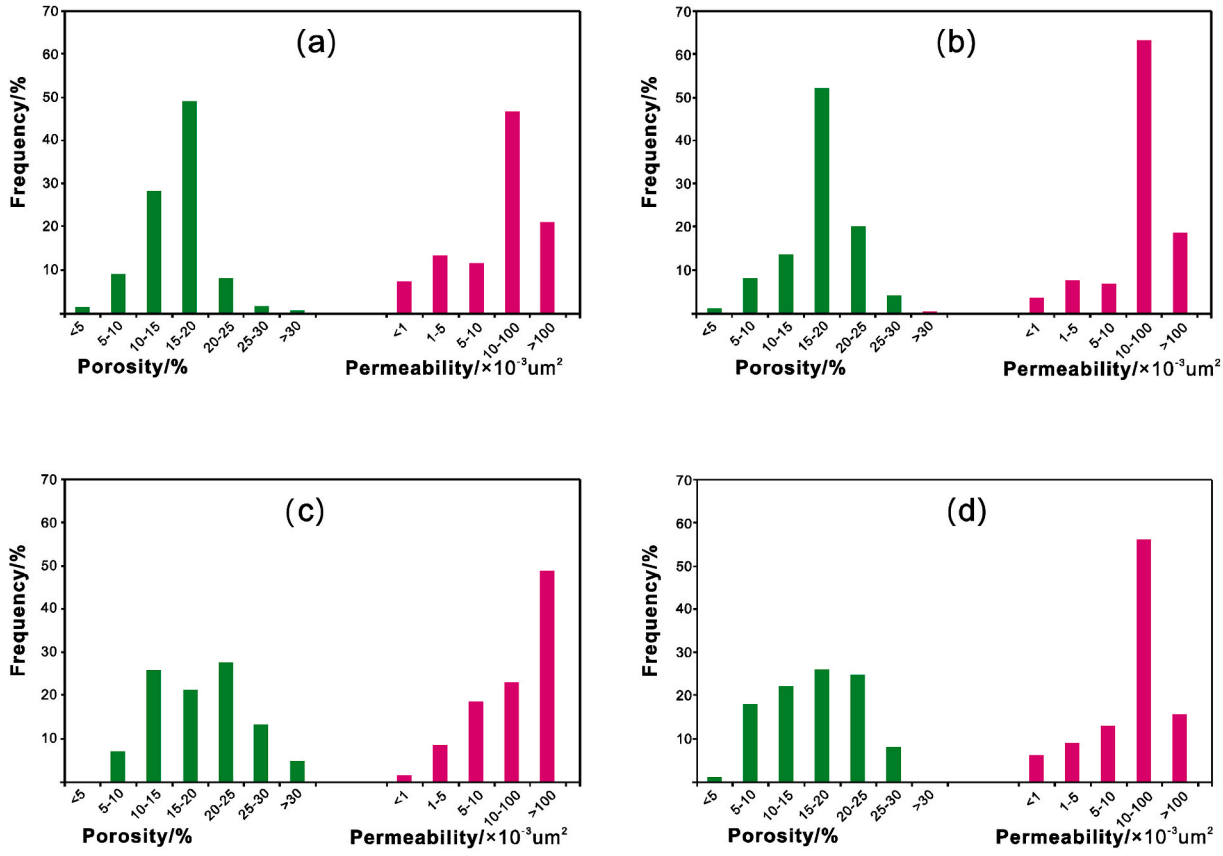

Fig. 7. Histograms of Porosity and permeability for the sandstones in Es3 Member (a), Es2 Member (b), Es1 Member (c) and Ed Formation (d), respectively.

porosity value greater than 10% account for more than 75% of Ed sandstone samples (Fig. 7d). More than 70% of Ed sandstone samples have relatively high permeability values greater than 10 × 10^{-3} μm^2 (Fig. 7d). Therefore, Ed sandstones have also been evaluated as medium porosity and medium permeability reservoir rocks. However, Ed Formation sandstones show better physical properties than those of Es Formation sandstones.

4.5.2. *Sandstone-to-strata ratio characteristics*

The sandstone-to-strata ratios in Es3 and Es2 members are relatively

low, usually <50%; particularly those in the Es3 Member are mostly <40% (Fig. 8a and b). Although the shallow lake dominated during the deposition of the Es1x Sub–member, a relatively short-term development of delta deposits took place before the extensive lacustrine transgression. As a result, sandstones were developed in the basal part of Es1x Sub–member (Es1xw Interval) (Fig. 1d). The Es1xw Interval, having a thickness of few dozens of meters, exhibits relatively low sandstone-to-strata ratios, usually <40% (Fig. 8c). The sandstone-to-strata ratios in Es1xs Interval are rather low and mostly less than 30%, except for a small area located to the southwest of the study area, which presents relatively high ratios in the range 30%–40% (Fig. 8d). The sandstone-to-strata ratios in the Es1s Sub–member are low and usually <40% (Fig. 8e). The Ed Formation is characterized by relatively lower sandstone-to-strata ratios, generally <35% (Fig. 8f).

5. Discussion

5.1. Source of crude oils

A study on the source of crude oils was conducted based on the oil classification and source rock evaluation. The relationship between crude oils and effective source rocks can be assessed from the distribution characteristics of biomarker compounds. The ternary diagram for the relative abundances of regular steranes C_{27}, C_{28}, and C_{29} shows that almost all samples selected from different source rocks and crude oils of different Paleogene strata fall into the same zone of mixed inputs of organic matter (Fig. 9). This indicates a dual organic matter input from aquatic organisms and terrigenous organic matter (Huang and Meinschein, 1979; Chen et al., 2014; Babangida et al., 2015). Thus, due to similar organic matter sources for all source rocks, the identification of the source of crude oils can be scarcely achieved based on the distribution characteristics of regular steranes alone.

Fig. 10a shows that most of the group I oil samples are characterized by relatively low C_{32} homohopane $S/(S + R)$ (usually <0.52) and low $Ts/(Tm + Ts)$ values (usually <0.40), implying that they vary from mainly immature to barely mature. Almost all group II oil samples have higher C_{32} homohopane $S/(S + R)$ (>0.5) and $Ts/(Tm + Ts)$ values (approximately 0.50), meaning they are mature (Fig. 10a). The C_{32} homohopane $S/(S + R)$ values of group III oil samples show a wide range, indicating immaturity to maturity, but all $Ts/(Ts + Tm)$ values are less than 0.45, suggesting immaturity (Fig. 10a). Most of the Es1x source rock samples have low C_{32} homohopane $S/(S + R)$ values (<0.5) and $Ts/(Tm + Ts)$ values (usually <0.35), indicating that they are generally immature (Fig. 10a). Almost all Es3x and Ek–Es4 source rock samples are characterized by relatively high C_{32} homohopane $S/(S + R)$ values (>0.54), indicating that they are mature (Fig. 10a). However, the $Ts/(Tm + Ts)$ values of the Es3x and Ek–Es4 source rock samples show a wide range, suggesting immaturity to maturity (Fig. 10a). Note that both Ts and Tm values are well known to be influenced by lithology, type, and maturation of organic matters (Moldowan et al., 1985). Therefore, some $Ts/(Tm + Ts)$ values of the Es3x and Ek–Es4 source rock samples were influenced by other factors, except the maturation of organic matter, resulting in the much lower values (Fig. 10a). Hence, it is believed that the Es3x and Ek–Es4 source rocks are primarily mature. Fig. 10b shows that there is a reasonably weak correlation and comparability, and the C_{29} sterane ααα $20S/(20S + 20R)$ and C_{29} sterane $\alpha\beta\beta/(\alpha\beta\beta + \alpha\alpha\alpha)$ values of the oil and source rock samples are less than the theoretical values. Therefore, these values are unfit to be used for the study on the oil-source relationship. Combining the above analysis of maturity parameters and Fig. 10a, it can be deduced that the group I oils mainly originated from Es1x source rocks, the group II oils were derived from either Es3x or Ek–Es4 source rocks or both, whereas the source of group III oils is fairly uncertain.

As displayed in Fig. 10c and d, the group I oils are believed to originate from Es1x source rocks. Compared to other samples, the samples from group I oils and Es1x source rocks have considerably higher $Pr/n\text{-}C_{17}$ and $Ph/n\text{-}C_{18}$ values (Fig. 10c), suggesting that the group I oils are derived from Es1x source rocks, not from Es3x and Ek–Es4 source rocks. This is further confirmed from the crossplot of gammacerane/C_{31} homohopane and Pr/Ph values, which shows that the distribution zone of the group I oil samples is very similar to that of the Es1x source rocks samples, but far away from the distribution zones of Es3x and Ek–Es4 source rocks (Fig. 10d). The group I oil samples and Es1x source rock samples are characterized by much higher gammacerane/C_{31} homohopane values and substantially lower Pr/Ph values, which respectively indicate strongly saline water conditions and anoxic depositional settings (Didyk et al., 1978; Fu et al., 1986; Peters and Moldowan, 1993; Chen et al., 2014). Compared to other samples, the group II oil samples and Ek–Es4 source rock samples have much lower $Pr/n\text{-}C_{17}$ and $Ph/n\text{-}C_{18}$ values, implying a good correlation (Fig. 10c). As shown in Fig. 10d, the group II oil samples fall into the distribution zone of Ek–Es4 source rock samples, which are characterized by relatively low gammacerane/C_{31} homohopane values and higher Pr/Ph values, suggesting slightly saline water conditions and weak anoxic depositional settings (Didyk et al., 1978; Fu et al., 1986; Peters and Moldowan, 1993; Chen et al., 2014). The crossplot of the $Pr/n\text{-}C_{17}$ and $Ph/n\text{-}C_{18}$ values indicates that the group III oil samples are located between the distribution zones of the Es1 and the Ek–Es4 source rock samples and close to the distribution zone of the Es3x source rock samples (Fig. 10c). Similarly, the crossplot of gammacerane/C_{31} homohopane and Pr/Ph values shows that the group III oil samples fall into the zone located between the distribution zone of the Es1 source rock samples and that of the Ek–Es4 source rock samples and close to the distribution zone of the Es3x source rock samples. The distribution zone of the group III oil samples represents saline water conditions and an anoxic depositional setting (Fig. 10d) (Didyk et al., 1978; Fu et al., 1986; Peters and Moldowan, 1993; Chen et al., 2014). Group I and group II oils are believed to be originated from Es1x and Ek–Es4 source rocks, respectively. Group III oils are chiefly distributed in the Tongkou area, located within the distribution zone of Es1x source rocks and adjacent to that of Ek–Es4 source rocks but away from that of the Es3x source rocks. Therefore, the group III oils are believed to be originated from both the Es1x and Ek–Es4 source rocks. Overall, the oil-source relationship is presented in Fig. 11.

Group I oils are distributed widely across the study area, mainly in the Gaoyang–Xiliu area (Fig. 3). Compared to the crude oil in other areas, the oils in the Gaoyang–Xiliu area (i.e., group I oils) are commonly characterized by much higher gravity and viscosity values, suggesting that these oils are of relatively low maturity. Low mature oils dominate the hydrocarbons derived from Es1x source rocks, and Es3x or Ek–Es4 source rocks generally produce mature oils (Ren, 2009; He et al., 2017a, 2017b, 2017c). This agrees with the above conclusions on the source of crude oils conducted based on geochemical data. Notably, a part of the Xiliu area lies adjacent to the Sub–trough, causing a small quantity of crude oils in this area to originate from the Es1x source rocks characterized by relatively higher maturities, so these oils have relatively lower gravity and viscosity values compared to the oils from other parts of Xiliu area (Fig. 5). Group II oils are distributed in the Yanling area (Fig. 3). The crude oils in the Yanling area (i.e., group II oils) generally have much lower gravity and viscosity values (Fig. 5), suggesting that they are mature oils. This matches the previous inference that group II oils are mainly derived from Ek–Es4 source rocks. Group III oils are distributed in the Tongkou area (Fig. 3). The gravity, viscosity, wax, and sulfur contents of the oils in the Tongkou area (i.e., group III oils) are between those in the Gaoyang–Xiliu and Yanling areas (Table 2; Fig. 5). This essentially supports the previous inference that the group III oils are a mixture of group I and II oils and that they resulted from the dual contributions of the Es1x and Ek–Es4 source rocks.

5.2. Controls of hydrocarbon accumulation

5.2.1. Source rock control on hydrocarbon accumulation

Three source rocks formed in and near the Lixian Slope: Es1x, Es3x,

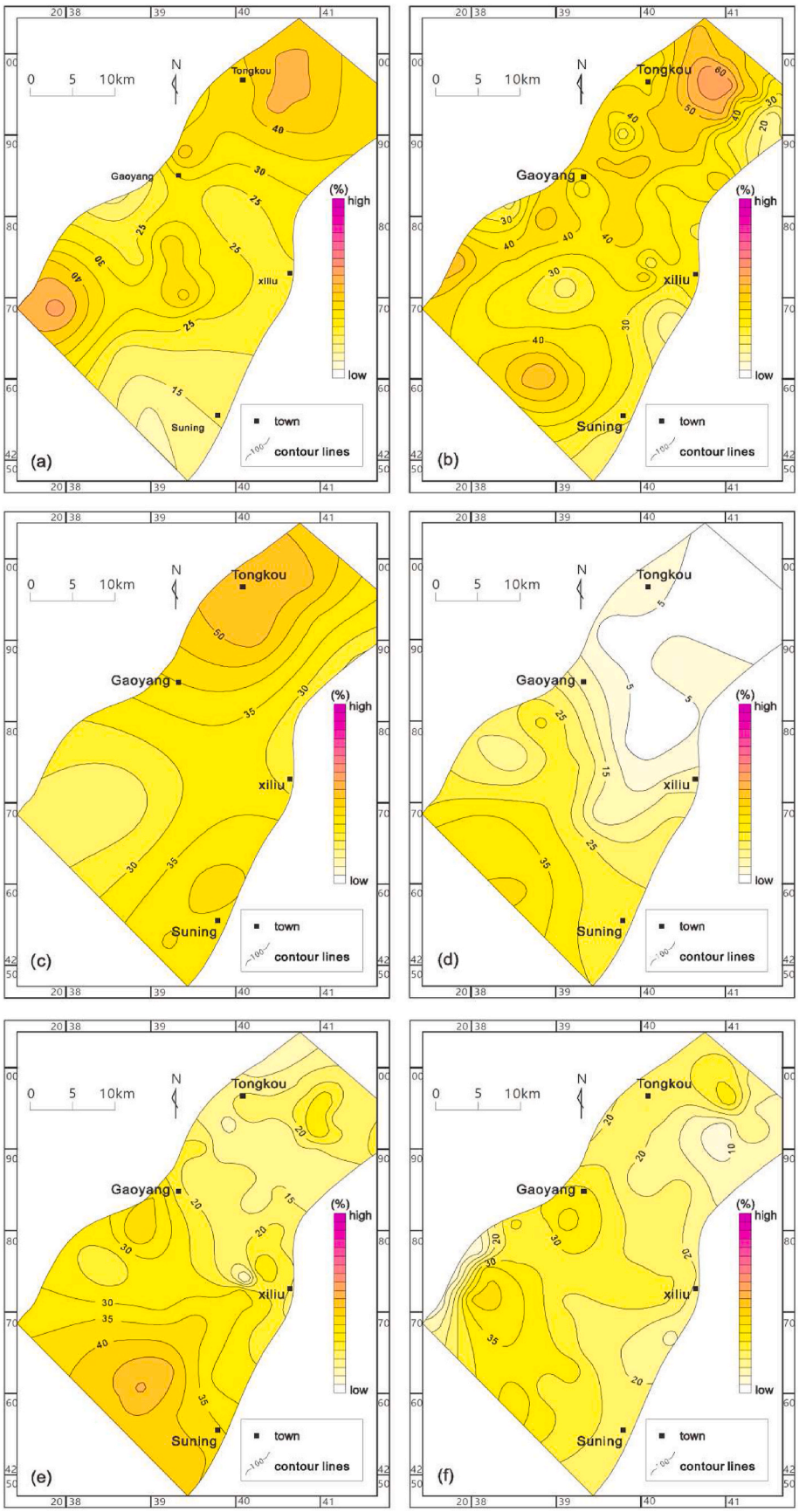

Fig. 8. Contour maps of sandstone-to-strata ratios for Es3 Member (a), Es2 Member (b), Es1xw Interval (c), Es1xs Interval (d), Es1s Sub-member (e) and Ed Formation (f), Lixian Slope.

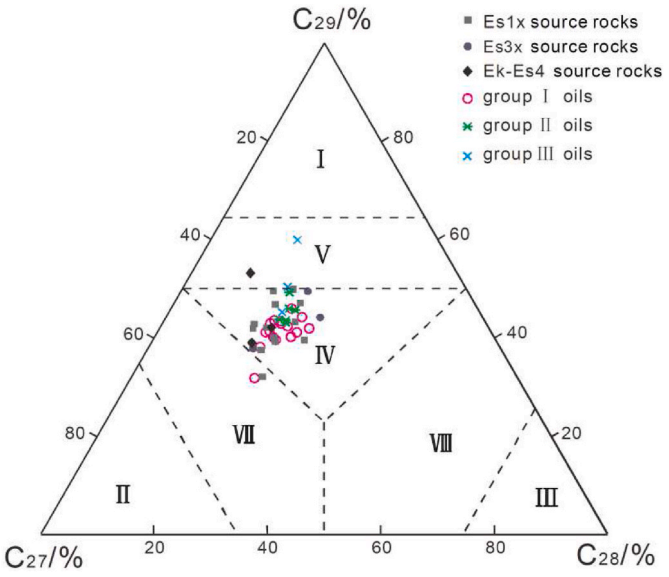

Fig. 9. Ternary diagram showing the relative abundances of regular steranes C_{27}, C_{28} and C_{29} of crude oils and source rocks samples, Lian Slope.

and Ek–Es4. It is well-known that effective source rocks hold the primary conditions for hydrocarbon accumulation, suggesting that the distributions of oil and gas reservoirs are bound to be controlled by the source rocks. Previous studies have pointed out that most of these source rocks have already entered the stage of hydrocarbon expulsion (Ren, 2009; Zhao et al., 2012; He et al., 2017a, 2017b, 2017c). This implies that these three sets of source rocks can supply hydrocarbons for traps. From the above discussion on oil-source correlation, the Es1x and Ek–Es4 source rocks act as the effective source rocks for Lixian Slope, and the former is the major source rock. Fig. 6 was generated by overlaying the discovered oil reservoirs and all sets of source rocks. This figure shows that all the oil reservoirs are distributed in the Es1x source rock zone, while the oil reservoirs discovered in the Yanling–Tongkou area are closely related to the Ek–Es4 source rocks and distributed in and near the Ek–Es4 source rock zone (Fig. 6). In addition, these two sets of source rocks, especially the Es1x source rocks, play an essential role in controlling the vertical distribution of oil and gas reservoirs. This has been further discussed in section 5.2.3.

5.2.2. Gradient control on hydrocarbon accumulation

Buoyancy is the principal migration force of hydrocarbons in the Lixian Slope (Zhao et al., 2012). The larger the dip-angle of the sandbody, the stronger is the force component of buoyancy, which in turn increases the speed of migration of oil and gas (Fu et al., 2014; Du, 2020). The developmental process of the Lixian Slope was characterized by considerably low gradients whose values are $\leq 1.00°$, implying that the force component of buoyancy was significantly weak. This is an important reason why the lateral migration distances of oils and gas in the Lixian Slope are relatively short.

5.2.3. Fault control on hydrocarbon accumulation

The faults play an essential role in migration and accumulation of oil and gas. They serve as barriers for lateral migration of oil and gas, and as favorable vertical channels for transporting oil and gas (Zhao et al., 2006; Xiong, 2006). Generally, active faults serve as major vertical pathways during the hydrocarbon accumulation stage (Hindle, 1997; Du et al., 2007; Liu et al., 2012).

The vertical transporting capacities of the faults in the Lixian Slope were evaluated based on the active history of faults discussed in section 4.2, combined with the hydrocarbon expulsion period of the effective source rocks. The previous section pointed out that the Es1x and Ek–Es4 source rocks are effective for the Lixian Slope. Li (2016) proposed that the Es1x and Ek–Es4 source rocks began expulsing hydrocarbons at around the Middle Minghuazhen and Early Dongying formational periods, respectively. The N–W trending faults ceased developing before the hydrocarbon expulsion period of these two sets of source rocks. This implies that the N–W trending faults hardly served as pathways for transporting the hydrocarbons generated by the Es1x and Ek–Es4 source rocks. The NNE–NEE trending faults were still developed during the deposition of the Ed Formation, suggesting that they had the capacities to act as vertical pathways for transporting the hydrocarbons generated by Ek–Es4 source rocks. However, these faults generally stopped developing during the hydrocarbon expulsion period of the Es1x source rocks, suggesting poor migration capacities for transporting the hydrocarbons generated by the Es1x source rocks. Given that the Es1x source rocks are the major source rocks in the Lixian Slope, the difficult upwelling of hydrocarbons derived from these source rocks is the primary factor that results in very few oil and gas reservoirs in the shallow strata overlying the Es1s Sub–member. Meanwhile, most of the NNE–NEE trending faults have cut across Es1x the source rocks, probably causing the Es1x source rocks to abut against the sandbodies that were developed on the other side of the faults. The fault throws are exceptionally low and usually less than 30 m. This facilitated the Es1x source rocks to have greater chances to abut against the Es2 and Es1 members on the other side of the faults (Fig. 12). Owing to this, the hydrocarbons in most areas of the Lixian Slope probably migrated and accumulated in the Es2 and Es1 members. This has been proved by the vertical distribution characteristics of the oil and oil–water layers in the slope. The discovered oil layers in the slope have been dominantly developed in the Es2 and Es1 members, with a few in the Es3 and Ed members (Fig. 13). The oil layers of the Es3 member, closely related to the Ek–Es4 source rocks, were mainly encountered in the north of the slope.

In addition, if the faults are developed well in a specific zone, it would be common that the horizontal distances between two faults are reasonably short. When the two faults have opposite inclination, the migrating oils in the sandbodies developed between them are usually blocked by the Es1x source rocks in the opposite wall of fault (Fig. 12a and b), then the fault-related oil and gas reservoirs form. The appearance of this situation largely results from the quite low fault throws, also causing these fault-related oil and gas reservoirs to be generally developed in these strata (Fig. 12a and b), which are near the Es1x source rocks in the vertical direction. These oil and gas reservoirs would form near the faults cut across Es1x the source rocks. Fig. 3a largely agrees with the above discussion and shows that the commercial oil wells and low-producing oil wells have been generally discovered near the NNE–NEE trending faults.

It can thus be inferred from the above discussions that the vertical distribution of the oil and gas reservoirs in the Lixian Slope is, to a great extent, a function of the major source rocks as well as the faults. In addition, the faults also play an important role in controlling the planar accumulation and enrichment of oil and gas reservoirs.

5.2.4. Control of sandbodies on hydrocarbon accumulation

The sandbodies typically serve as lateral pathways for transporting oils and gas. The average porosity and permeability values of the Es Formation sandstones are approximately 15%–18% and 70×10^{-3}–80×10^{-3} μm^2, respectively (Fig. 7). The physical properties of the Ed Formation sandstones are enhanced compared to those of the Es Formation sandstones and have average porosity, and permeability values are approximately 19.0% and 440×10^{-3} μm^2, respectively (Fig. 7). Therefore, the medium porosity and permeability reservoir rocks dominate the Lixian Slope Paleogene strata, indicating that the Paleogene sandstones exhibit good transport performance.

In the case of a limited number of wells, the sandstone-to-strata ratios are considered more practical tools for evaluating the connectivity of sandbodies (Qiu, 1990; Lin et al., 1995; Lei et al., 2013; Fu et al., 2014). Allen (1978) researched the connectivity of sandbodies based on

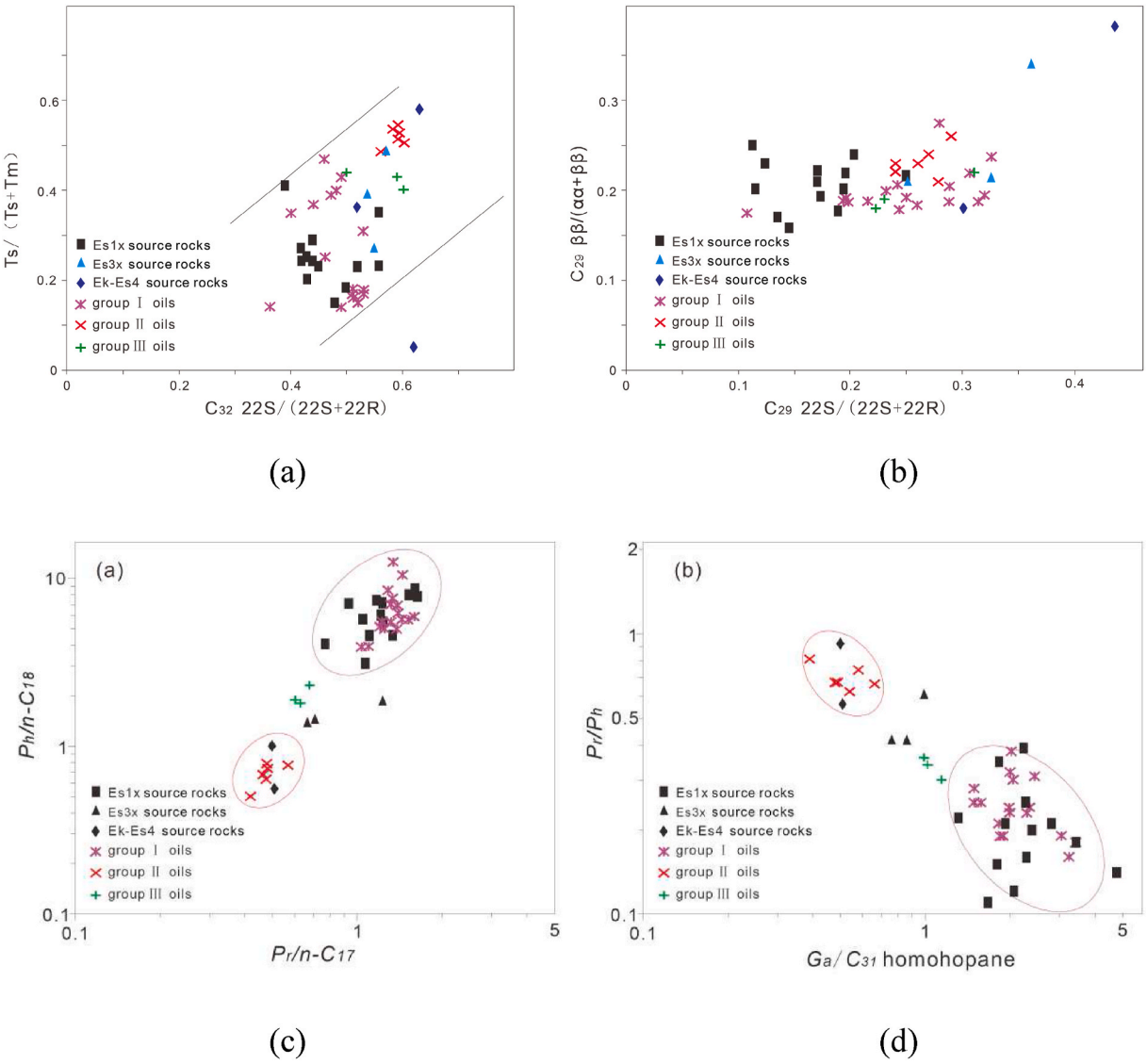

Fig. 10. (a) Cross plot of *Ts/(Tm + Ts)* versus C_{32} *homohopane S/(S + R)*, (b) of C_{29} *sterane ααα 20S/(20S + 20R)* versus C_{29} *sterane αββ/(αββ+ααα),* (c) of *Pr/n-*C_{17} versus *Ph/n-*C_{18}, and (d) of *Pr/Ph* versus *Ga* (*gammacerane*)/C_{31} *homohopane* of crude oils and source rocks samples, Lixian Slope.

the sandstone-to-strata ratios and proposed a threshold value of 0.50. In other words, if the sandstone-to-strata ratio is lower than this threshold value, the sandbodies will be essentially disconnected. With the increase in the ratio, as it surpasses this threshold value, the chances for sandbodies to superimpose each other increases rapidly, thereby increasing the probabilities of sandbody connectivity. In addition, some researchers have pointed out that the sandbodies will have good connectivity if the sandstone-to-strata ratios are greater than 50%; otherwise, have relatively poor connectivity (Qiu, 1990; Lin et al., 1995). In the Paleogene of the Lixian Slope, the Es3 Member, Es2 Member, Es1xw Interval, Es1xs Interval, Es1s Sub–member, and Ed Formation show relatively low sandstone-to-strata ratios of generally less than 40%, 50%, 40%, 30%, 40%, and 35%, respectively. The sandstone-to-strata ratios for different Paleogene strata are lower than the proposed threshold value (0.5), suggesting that the connectivity of sandbodies in the Paleogene of the Lixian Slope is generally poor. Thus, they have an outstanding possibility to pinch out in relatively short distances. This is another important factor that causes the lateral migration distance of oils and gas to be short.

Most NNE–NEE trending faults cut across the Es1x source rocks, commonly causing the hydrocarbons generated by these source rocks to enter laterally into the sandbodies developed on the other side of the fault. Given that the faults are characterized by exceptionally weak vertical transporting capacities, this is the primary pattern in the slope that the oil and gas entered the sandbodies from source rocks in Lixian Slope (Fig. 12). As the Paleogene sandbodies have poor connectivities, the lateral migration distances of hydrocarbons are most likely to be relatively short and accumulate near these faults (Fig. 12c and d). Thus, the planar accumulation and enrichment of the oil and gas reservoirs in Lixian Slope is chiefly controlled by sandbodies and faults.

5.3. Hydrocarbon accumulation models

The abnormal pressure is nearly absent in the slope (Zhao et al., 2012). Thus, the current fluid potential distribution characteristics of a certain stratum primarily depend on its structural feature (Hubbert, 1953; Ren et al., 2019). Overall, the structural feature of the Lixian Slope did not undergo obvious change during its entire developmental history, displaying a high inheritance. This means that each stratum's current fluid potential distribution characteristics resemble each other. Therefore, the Es1x Sub–member, the essential target layer of this study, has been chosen for the representative stratum. Fig. 14 shows the current

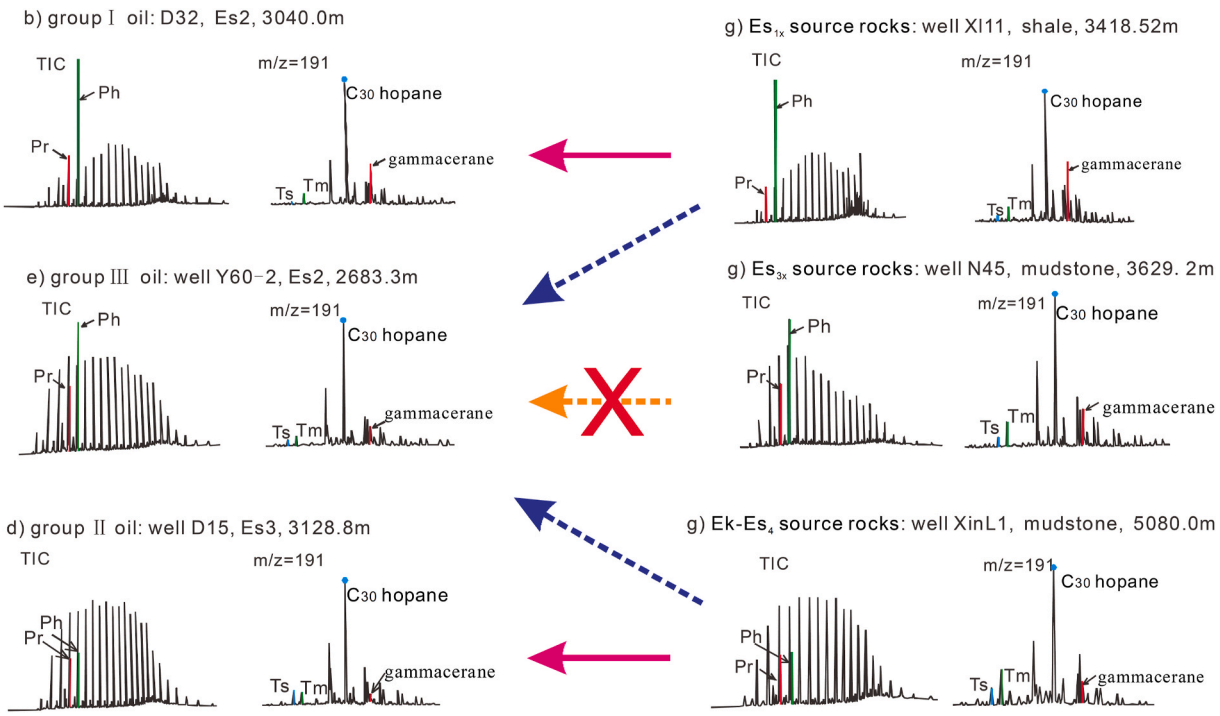

Fig. 11. The GC-MS analysis results of representative different crude Oil groups and source rocks samples, and the oil source relations.

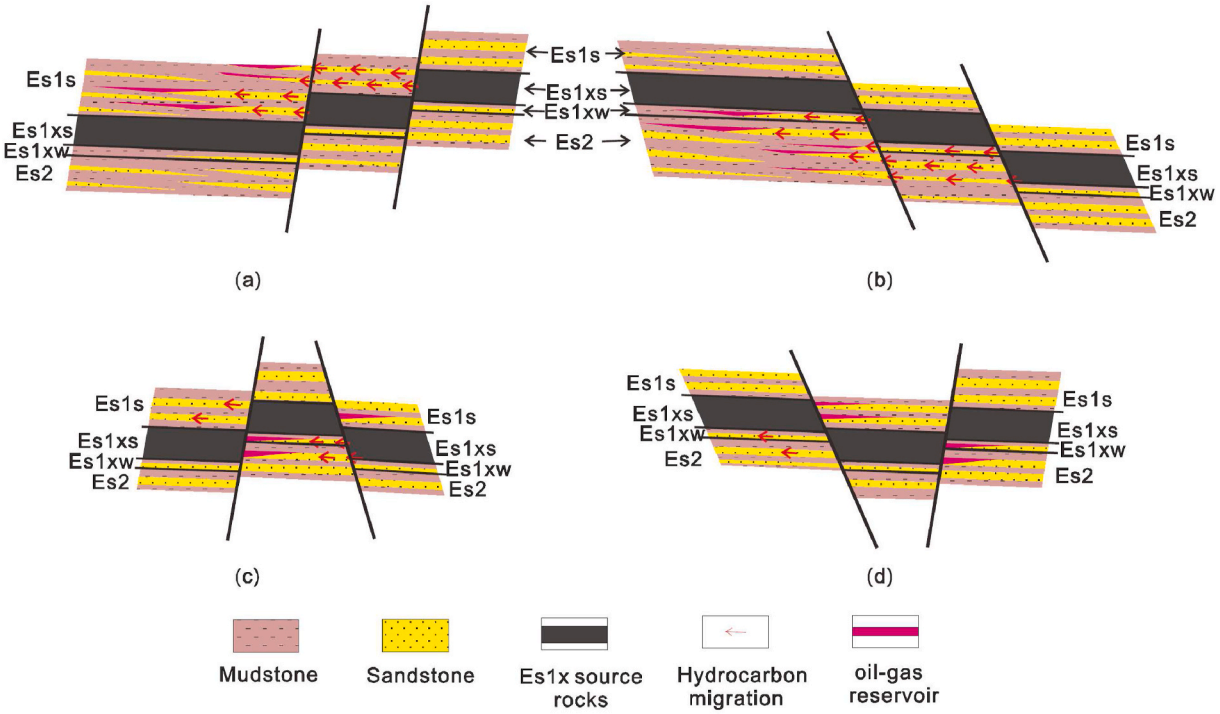

Fig. 12. Common distributions of strata on both sides of faults (a, b, c, d), Common patter that the hydrocarbons of migration and accumulation, Lixian Slope.

fluid potential distribution characteristics of the Es1x Sub–member. Overall, the trough belt always has the highest fluid potentials, and the outer slope is commonly characterized by the lowest fluid potentials (Fig. 14). It is well known that oil and gas migrate from high fluid potentials to low fluid potentials (Hubbert, 1953; He et al., 1993). The oil and gas in Lixian Slope migrate from east to west (Fig. 14). Besides, due to the weak terrain deformations, the oil and gas migration directions are almost parallel to the inclination of the slope. Though some small structural high points can lead to slight changes in the oil and gas direction, the macroscopical migration direction of oil and gas is basically unchanged. The dominant migration direction of oil and gas in the Lixian Slope is the northwest direction (Fig. 14).

The Es1x and Ek–Es4 source rocks began to expulse hydrocarbons roughly after the Dongying formational period (Li, 2016). The Lixian Slope has not undergone any major tectonic activity post the deposition of the Dongying Formation, leaving the structural characteristics of the

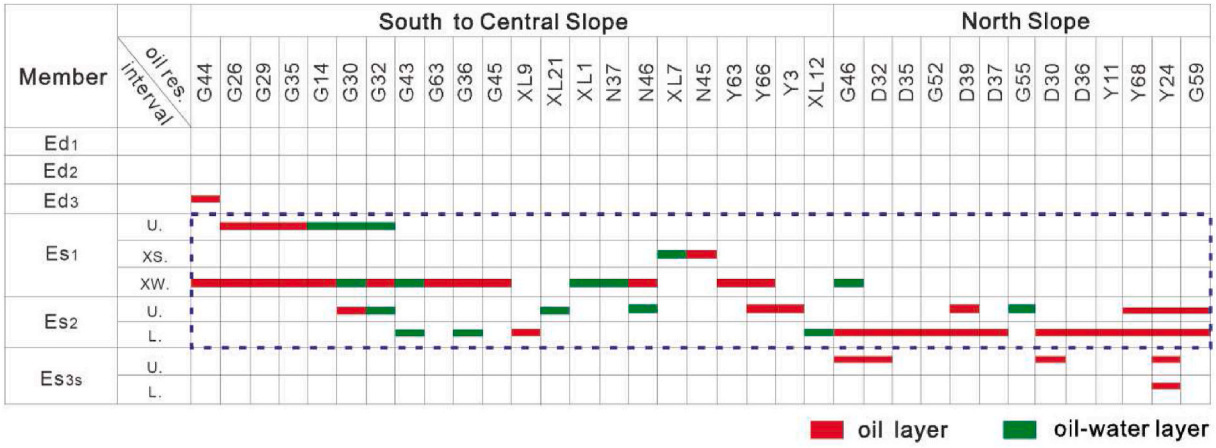

Fig. 13. Vertical distributions of oil-gas reservoirs in Paleogene, Lixian Slope. L.: lower part of Member; U.: upper part of Member; XW.: Es1xw Interval; XS.: Es1xs Interval.

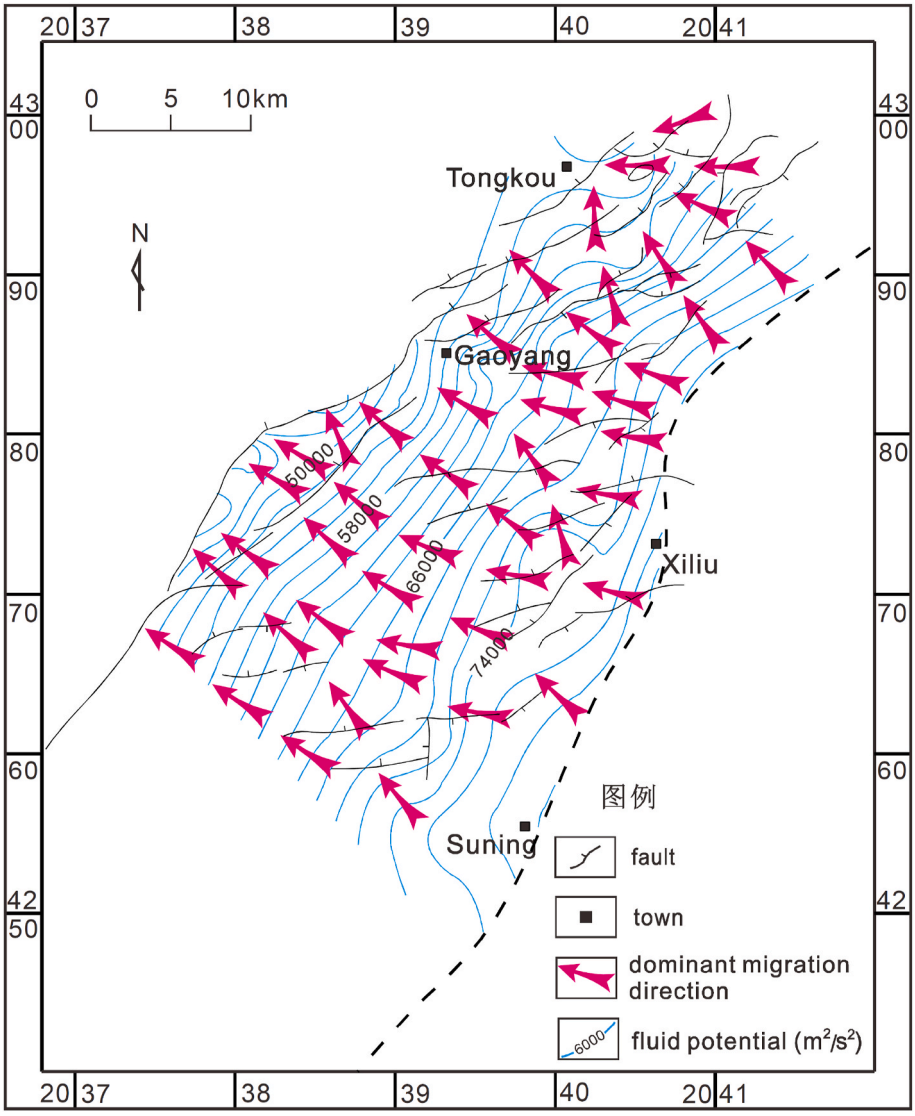

Fig. 14. Overlayed map shows the current fluid potential distribution characteristics of Es1x, and the distribution characteristics of dominant migration direction, Lixian Slope (modified after Ren, 2009).

Lixian Slope unchanged (Ren, 2009; Chen, 2019). This suggests that the current structural background of the Lixian Slope is exceedingly similar to that during the hydrocarbon accumulation period. Thus, studies on hydrocarbon accumulation models were conducted considering the current structural background of the Lixian Slope.

The results of the oil-source correlation show that the source rocks in the trough of Baxian Sag, located to the north of the Lixian Slope, supply oils for the northernmost area of the slope. However, the oils in most areas of the Lixian Slope came from Es1x source rocks. Thus, there are some different hydrocarbon accumulation models in the Lixian Slope. The hydrocarbon accumulation models in the north of the slope are only suitable for small areas, are occasional, and have limitations. They cannot be considered as the representative hydrocarbon accumulation modes in the weak structure slope belt. Therefore, further discussion on these hydrocarbon accumulation models is not conducted. Based on the research on the characteristics of source rocks, reservoir rocks, and transport systems, the discussion on oil-source correlations, controls on hydrocarbon accumulation, the dominant migration direction, and the analyses of their tectonic background during the hydrocarbon accumulation stage, the representative hydrocarbon accumulation model suitable for most areas of the Lixian Slope was proposed. This model can reflect the influences of weak tectonic activity on hydrocarbon accumulation characteristics and control factors. This hydrocarbon accumulation model is illustrated in Fig. 15.

Generally, a weak tectonic slope is characterized by exceptionally low gradients throughout its entire development. Thus, even a relatively small rise of water would cause the lake level to extend for a long distance, respectively. As a result, the source rocks usually develop well in the weak tectonic slope. Similarly, in the Lixian Slope, the Es1x source rocks are distributed widely. In this hydrocarbon accumulation model, the crude oils of the Paleogene strata in most parts of the study area originated from the Es1x source rocks. Most NNE–NEE trending faults cut across the Es1x source rocks, usually enabling the hydrocarbons from Es1x source rocks to directly enter the sandbodies on the other side of these faults (Fig. 15). In this hydrocarbon accumulation model, this is the dominant pattern that the oil and gas entered the sandbodies from source rocks. In addition, a small part of hydrocarbons generated by Es1x source rocks would migrate into the sandbodies directly connected to these source rocks (Fig. 15). The Paleogene sandbodies in the Lixian Slope are characterized by relatively poor connectivities. Therefore, the sandbodies in the study area would have great chances to gradually pinch out along the updip direction in a relatively short distance, causing these sandbodies to be blocked by mudstones (Fig. 15). When the oil and gas entered these sandbodies, the lithologic oil and gas reservoirs would have formed. In addition, due to the low fault throws, the sandbody was usually blocked by the Es1x source rocks on the other side of the faults (Fig. 15). This situation mainly occurred in the area where the faults were thick. Thus, the fault-related oil and gas reservoirs more easily formed in these areas. Overall, the oil and gas reservoirs were usually developed near the faults cut across Es1x the source rocks. In the proposed hydrocarbon accumulation model, updip pinch-out lithological oil and gas reservoirs and faulted-related oil and gas reservoirs are dominant. As discussed in the previous section 5.2.3, the hydrocarbons generated by the Es1x source rocks mostly entered and migrated into the sandbodies of the strata, such as the Es2 and Es1 members, which are near to the Es1x source rocks in the vertical direction. Thus, the oil and gas reservoirs mainly formed in the Es2 and Es1 members in this model (Fig. 12; Fig. 15).

5.4. Recommendations for future exploration

The study of the controls and geological models of hydrocarbon accumulation in the Lixian Slope shows that the Es2 and Es1 members, especially the region between the upper part of the Es2 Member and the low part of the Es1s Sub–member, are the target intervals for future exploration. Apart from these, in the north of the slope, the deeper Paleogene strata, even buried hills have a high potential for oil and gas exploration. Determining favorable exploration locations on such gentle slopes largely depends on the source rocks, sandbodies, and faults. The previous studies have examined the source rocks and fault characteristics in detail. However, now it is important to emphasize further studies of sandbodies. The discussion presented in previous sections reveals that the Paleogene sandbodies in the Lixian Slope generally have relatively poor connectivity, thus greatly increasing the possibility of the sandbodies to pinch out. This is proved to some extent by the feature that the lithological and faulted-lithological traps are dominant in this slope. Sequence stratigraphy has a significant advantage in determining the spatial distribution of sandbodies and is the most commonly used method for predicting lithologic traps (Law and Curtis, 2002; Catuneanu et al., 2009; Cao et al., 2010; Zahid et al., 2016). The cognition of the lateral connectivity of sandbodies and the spatial developmental characteristics of the updip pinch-out sandstones in the slope will become much more evident with the help of sequence stratigraphy. In addition, the carbonate reservoir rocks and beach bar sandstones, generally intercalated by the Es1x source rocks, possess good physical properties. This suggests that the Es1xs Interval bears desirable potential for oil and gas exploration. The study of sequence stratigraphy and sedimentology is also helpful for the oilfield workers to find out the carbonate reservoir

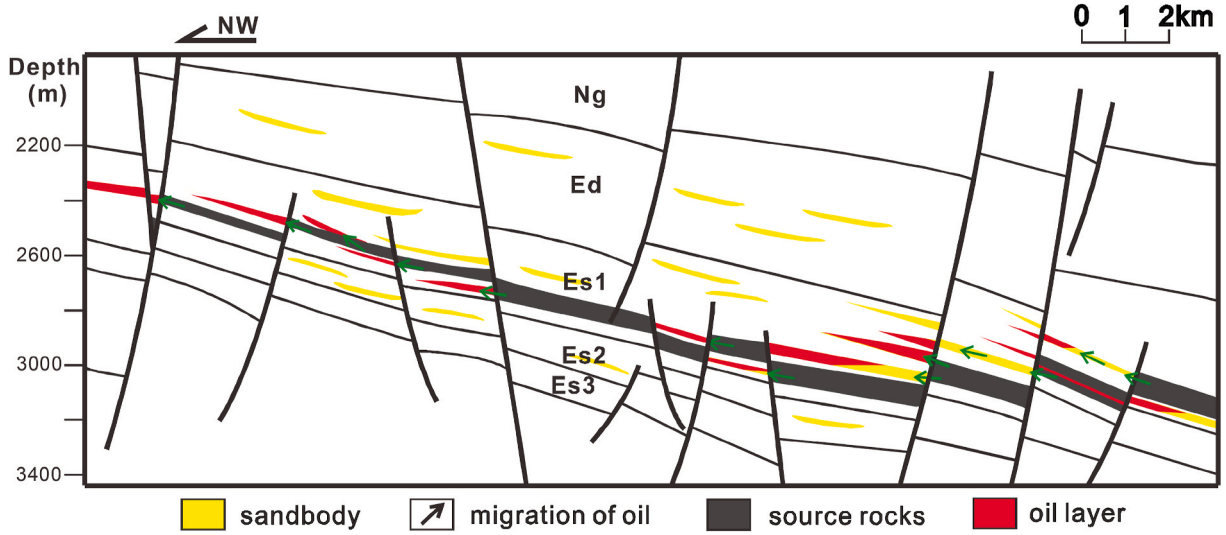

Fig. 15. Representative hydrocarbon accumulation model, Lixian slope.

rocks and beach bar sandstones. Thus, it is essential to carry out detailed stratigraphic and sedimentological studies of the region to plan better exploration operations.

6. Conclusions

(1) The Lixian Slope has always been a gentle slope of exceptionally low gradient, with values less than 1.00° during its developmental stage. This is an important one of reasons why the lateral migration distances of oils and gases in the Lixian Slope are relatively short.
(2) The faults in this type of slope are usually underdeveloped. Most of the faults exhibited extremely low fault throws of <30 m and relatively short durations of tectonic activities throughout their developmental stages. The faults in the Lixian Slope hardly acted as vertical pathways for transporting hydrocarbons generated by the Es1x source rocks.
(3) The sandstone-to-strata ratios of different Paleogene strata are typically <40%, except for those of the Es2 Member, which are <50%, suggesting that the sandbodies have poor connectivities. This essentially caused the lateral migration distances of hydrocarbons to be relatively short.
(4) The Es1x and Ek–Es4 source rocks, Es1x in particular, act as the major source rocks in the slope and play important roles in controlling the planar distribution of oil and gas reservoirs. The faults and source rocks display major controls on the vertical distribution of oil and gas reservoirs. Vertically, the oil and gas reservoirs in the Lixian Slope were commonly developed in the Es2 and Es1 members. The sandbodies and faults, and significant contributions from exceptionally low slope gradients, controlled the planar accumulation and enrichment of oil and gas reservoirs. In the plane, the oil and gas reservoirs have been mainly discovered near the faults that had cut across Es1x the source rocks.
(5) A representative hydrocarbon accumulation model was proposed. In this model, the oils mainly originated from Es1x source rocks. Most of the oils generated by Es1x source rocks entered into the sandbodies in the opposite walls of faults. Generally, these oils migrated just for relatively short distances due to the poor connectivity of sandbodies. Thus, the updip pinch-out lithological oil and gas reservoirs are common. Besides, some oils were usually blocked by Es1x source rocks in the opposite walls of faults; therefore, the fault-related oil and gas reservoirs were also well developed. These oil and gas reservoirs mainly formed near the faults, which had cut across the Es1x source rocks. Besides, as most of the fault throws are extremely low, these oil and gas reservoirs generally formed in these strata, such as Es2 and Es1 members, which are near the Es1x source rocks in a vertical direction.

Declaration of competing interest

The authors declare that they have no known competing financial interests or personal relationships that could have appeared to influence the work reported in this paper.

Acknowledgements

This research was financially supported by the Huabei Oilfield Branch. We thank the Huabei Oilfield Branch for allowing us to observe and sample the core materials. We are grateful to the College of Geoscience, China University of Petroleum (Beijing) and the State Key Laboratory of Organic Geochemistry at the Guangzhou Institute of Geochemistry for providing us with the research facilities.

References

Allen, J.R.L., 1978. Studies in fluviatile sedimentation: an exploratory quantitative model for the architecture of avulsion controlled alluvial suites. Sediment. Geol. 21 (2), 129–147.
Babangida, M.S., Wan, H.A., Abubakar, M.B., Mohammed, H.H., Khairul, A.M., Adebanji, K.A., 2015. Organic geochemical characteristics of Cretaceous Lamja Formation from Yola Sub–basin, Northern Benue Trough, NE Nigeria: implication for hydrocarbon–generating potential and paleodepositional setting. Arabian J. Geosci. 8, 7371–7386.
Basu, H., Dandele, P.S., Srivastava, S.K., 2021. Sedimentary facies of the Mesoproterozoic Srisailam Formation, Cuddapah basin, India: implications for depositional environment and basin evolution. Mar. Petrol. Geol. 133, 105242.
Cao, R.C., Li, J.H., Lu, S.F., Zhang, D.Z., Liu, Q.H., Chen, X.M., Zhao, Y., Hu, S.M., 2010. Cretaceous sequence stratigraphy and sedimentary evolution of Huhehu depression in Hailar Basin. J. Jilin Univ. (Earth Sci. Ed.) 27 (2), 306–311.
Catuneanu, O., et al., 2009. Toward the standardization of sequence stratigraphy. Earth Sci. Rev. 92, 1–33.
Chen, J., 2019. Tectonic Evolution of the Buried Hills in the Western Slope of Shulu Sag and its Petroleum Geological Significance. Degree's thesis. Northwest University (EastChina) (in Chinese with English abstract).
Chen, W.B., Fu, X.G., Tan, F.W., Feng, X.L., 2014. Geochemical characteristics of biomarkers of the upper triassic source rocks from tumengela formation in Qiangtang Basin of Tibet. Geoscience 28 (1), 216–223 (in Chinese with English abstract).
Didyk, B.M., Simoneit, B.R.T., Brassell, S.C., Eglinton, G., 1978. Organic geochemical indicators of palaeoenvironmental conditions of sedimentation. Nature 272, 216–222.
Donaldson, A.C., 1974. Pennsylvanian sedimentation of central Appalachians, special papers. Geol. Soc. Am. 148, 47–48.
Du, Z.J., 2020. Mechanism of "high-speed braking" effect on heavy oil formation during hydrocarbon migration: a case study of the eastern part of southern slope of Dongying Sag, Bohai Bay Basin. Petrol. Geol. Exp. 42 (1), 126–131 (in Chinese with English abstract).
Du, C.G., Hao, F., Zou, H.Y., Zhang, S.L., Fu, X.F., 2007. Progress and problems of faults conduit systems for hydrocarbon migration. Bull. Geol. Sci. Technol. 26 (1), 51–56 (in Chinese with English abstract).
Fu, J.G., Sheng, P., Peng, S.C., Brassell, S.C., Eglington, G., 1986. Peculiarities of salt lake sediments as potential source rocks in China. Org. Geochem. 10, 119–127.
Fu, G., Sun, T.W., Lv, Y.F., 2014. An Evaluation method of oil-gas lateral transporting ability of fault-sandstone configuration in Nanpu Depression. J. China Univ. Min. Technol. 43 (1), 79–87 (in Chinese with English abstract).
Gao, C.H., Zha, M., Ge, S.Q., Chen, L., Zhao, X.Z., Jin, F.M., 2014. The Jizhong Depression Main controlling factors and models of hydrocarbon accumulation in weak structural belts of oil-rich sags, the Jizhong Depression. Oil Gas Geol. 35 (5), 595–600 (in Chinese with English abstract).
Gu, W.B., 2013. The Research on the Oil-Gas Reservoir-Forming Condition of Dujiatai Buried Hill in the Western Slope of Western Sag in Liaohe Depression. Degree's thesis. Northeast Petroleum University (in Chinese with English abstract).
Hanson, A.D., Zhang, S.C., Moldowan, J.M., et al., 2000. Molecular organic geochemistry of the Tarim basin, Northwest China. AAPG Bull. 84, 1109–1128.
He, H., 2010. High-resolution Sequence Stratigraphy and the Characteristics of Hydrocarbon Accumulation in the West Slope of Songliao Basin. Degree's thesis. China University of Geosciences (Beijing (in Chinese with English abstract).
He, Z., Xia, D., 2017. Hydrocarbon Migration and Trapping in Unconventional Plays: AAPG Annual Convention & Exhibition. Search and Discovery. Houston Article #10968.
He, S., Tang, Z.H., Chen, R.H., 1993. Application of mathematical model of secondary hydrocarbon migration as a buoya-driven separate phase flow in Liaodong gulf. Earth Sci. J. China Univ. Geosci. 18, 612–620 (in Chinese with English abstract).
He, B., Li, J.Z., Tang, Z.J., Li, P., Wang, L., Shang, X.Y., 2017a. High-resolution sequence stratigraphy, sedimentology and reservoir quality evaluation of the Yaojia formation in the Longxi area of the western slope, songliao basin, China. Mar. Petrol. Geol. 88, 511–530.
He, F.G., Gao, X.Z., Zhao, X.Z., Yang, D.X., Lu, X.J., Liu, J.W., Dong, X.Y., Wang, H.L., Wu, D.S., 2017b. Geochemical characteristics of the lower part of Shayi member in Lixian slope, Raoyang sag, Bohai Bay Basin, northern China: implications for organic matters origin, thermal maturity and depositional environment. Geochem. Int. 55 (12), 1140–1153.
He, F.G., Gao, X.Z., Zhao, X.Z., Yang, D.X., Wang, Q., Fan, B.D., Wang, H.L., Liu, J.W., Wu, D.S., 2017c. The lower part of the first member of the Shahejie formation (Es1x) as a source rock for oil found in Lixian Slope, Raoyang Sag, Bohai Bay Basin, Northern China. Arabian J. Geosci. 10 (5), 101.
Hindle, A.D., 1997. Petroleum migration pathways and charge concentration: a three dimensional model. AAPG (Am. Assoc. Pet. Geol.) Bull. 81 (9), 1451–1481.
Horne, J.C., Ferm, J.C., Caruccio, F.T., Baganz, B.P., 1976. Depositional models in coal exploration and mine planning in appalachian region. AAPG Bull. 62 (12), 2379–2411.
Huang, W.Y., Meinschein, W.G., 1979. Sterols as ecological indicators. Geochem. Cosmochim. Acta 43, 739–745.
Hubbert, M.K., 1953. Entrapment of Petroleum under hydrodynamic conditions. AAPG (Am. Assoc. Pet. Geol.) Bull. 37, 1954–2026.
Jiang, J.W., Xiao, M.H., Wang, J.P., Hu, S.K., 2016. Detailed reservoir architecture of fan-delta front in Shuanghe Oilfield,Biyang depression. Fault-Block Oil Gas Field 23 (5), 560–568 (in Chinese with English abstract).

Law, B.E., Curtis, J.B., 2002. Introduction to unconventional petroleum systems. AAPG Bull. 86 (11), 1851–1852.
Lei, Y.H., Luo, X.R., Zhang, L.K., Song, C.P., Cheng, M., 2013. Quantitative characterization of Shahejie Formation sandstone carrier connectivity of the eastern part of south slope in Dongying sag. Acta Petrol. Sin. 34 (4), 692–700 (in Chinese with English abstract).
Li, P.L., 2001. Research on Rule of Oil-Gas Migration and Accumulation in the Gentle Slope of Terrestrial Fault Basin. Degree's thesis. Lanzhou Institute of Geochemistry, Chinese Academy of Sciences (in Chinese with English abstract).
Li, D.M., 2010. Research on Hydrocarbon Enrichment Rules of Gentle Slope in Half Graben Basin—The Example of Shulu West Slope. Degree's thesis. China University of Geosciences, Beijing (in Chinese with English abstract).
Li, H., 2016. Research on Characteristics of Hydrocarbon Accumulation in Lixian Slope, Raoyang Sag. Degree's thesis. China University of Petroleum (Beijing (in Chinese with English abstract).
Li, P.L., et al., 2003. Petroleum Geology and Exploration of Continental Fault Basin. Petroleum Industry Press, Beijing, pp. 1–96 (in Chinese with English abstract).
Lin, K.X., Zhang, C.M., Liu, H.B., Lei, B.J., Qu, P.Y., Ma, W.X., Lei, B.Z., Tang, R.Y., 1995. Establishment of geological model for labyrinth diffluence channel sand bodies in Youshashan oilfield, Qinghai. Oil Gas Geol. 16 (2), 98–109 (in Chinese with English abstract).
Liu, Z., Lv, Y.F., Sun, Y.H., Li, Y.B., Zhang, D.W., 2012. Characteristics and significance of syngenetic fault segmentation in hydrocarbon accumulation:an example of Yuanyanggou fault in western sag, Liaohe depression. J. China Univ. Min. Technol. 41 (5), 793–799 (in Chinese with English abstract).
Mao, T.T., 2012. Sequence Stratigraphy of Wen'an Slope in Baxian Depression. Degree's thesis. Yangtze University (in Chinese with English abstract).
Miao, Q.Y., 2018. The Cenozoic Structural Style and Evolution of Eastern Jizhong Depression. Degree's thesis. China University of Petroleum (Beijing (in Chinese with English abstract).
Moldowan, J.M., Seifert, W.K., Gallegos, E.J., 1985. Relationship between petroleum composition and depositional environment of petroleum source rocks. AAPG Bull. 69, 1255–1268, 1985.
Peters, K.E., Moldowan, J.M., 1993. The Biomarker Guide: Interpreting Molecular Fossils in Petroleum and Ancient Sediments. Prentice–Hall, Englewood Cliffs.
Qi, J.F., Yang, Q., 2010. Cenozoic structural deformation and dynamic processes of the Bohai Bay basin province, China. Mar. Petrol. Geol. 27, 757–771.
Qiu, Y.N., 1990. A proposed flow-diagram for reservoir sedimentological study. Petrol. Explor. Dev. 1, 85–90 (in Chinese with English abstract).
Qiu, R.H., Li, L.S., Zhang, Y.H., Tian, X.M., Zhu, J.X., 2006. Control on hydrocarbon accumulation and exploration techniques in the Northern Slope belt of Biyang Depression. J. Oil Gas Technol. (J. Jianghan Petroleum Inst.) 28 (2), 39–41 (in Chinese with English abstract).
Ren, J.S., 1994. The continental tectonics of China. Bull. Chin. Acad. Geol. Sci. 3, 5–13 (in Chinese with English abstract).
Ren, X.J., 2009. Research on Hydrocarbon Enrichment Rules of Gentle Slope in Half Graben Basin: the Example of Lixian Slope in Jizhong Depression. Degree's thesis. China Unversity of Geosciences, Beijing) (in Chinese with English abstract).
Ren, C.Q., He, F.G., Gao, X.Z., Wu, D.S., Yao, W.L., Tian, J.Z., Guo, H.P., Huang, Y.X., Wang, L., Feng, H., Li, J.W., 2019. Prediction of exploration targets based on integrated analyses of source rock and simulated hydrocarbon migration direction: a case study from the gentle slope of Shulu Sag, Bohai Bay Basin, northern China. Geosci. J. 23 (6), 977–989.
Rong, Q.H., Pu, Y.G., Song, J.G., Xu, L., Shao, Y., 2001. Distribution characteristics and descriptive models of slope belt reservoir in dustpan-like sag—taking southern slope in southwest of Dongying sag as an example. Petrol. Geol. Recov. Effic. 8 (2), 25–28 (in Chinese with English abstract).
Seifert, W.K., Moldowan, J.M., 1978. Applications of steranes, terpanes and monoaromatics to the maturation, migration and source of crude oils. Geochim. Cosmochim. 42, 77–95.
Xiao, P., 2007. Characteristics and Evaluation of Middle Ordovician Marine Carbonate Source Rocks in Bohai Bay Basin. Degree's thesis. China University of Geosciences (Beijing (in Chinese with English abstract).
Xiong, W., 2006. Macroscopic framework and constitution characteristics of the transportation system in downfaulted basin—an example from Dongying Sag, Shengli Oilfield. Petrol. Explor. Dev. 33 (4), 474–478 (in Chinese with English abstract).
Xiong, W., 2009. Research on the Transmission System in the Southern Slopeof Dongying Sag. Degree's thesis. Degree's thesis. China University of Petroleum (EastChina) (in Chinese with English abstract).
Yang, Y.T., Xu, T.G., 2004. Hydrocarbon Habitat of the Offshore Bohai basin, China. Mar. Petrol. Geol. 21, 691–708.
Yang, W.R., Qian, Z., Zhang, X., Zhu, P., Fan, C.X., 2008. Accumulation characteristics in Wen'an slope belt in Jizhong depression. Lithol. Reserv. 20 (3), 49–52 (in Chinese with English abstract).
Zahid, M.A., Dong, C., Lin, C., Gluyas, J., Jones, S., Zhang, X., Munawar, M.J., Ma, C., 2016. Sequence stratigraphy, sedimentary facies and reservoir quality of Es4s, southern slope of Dongying depression, Bohai bay Basin, East China. Mar. Petrol. Geol. 77, 448–470.
Zhang, J.Z., 2006. The Forming Mechanism of Gentle Slope and Reservoir-Forming Law in Jiyang Depression. Degree's thesis. Guangzhou Institute of Geochemistry, Chinese Academy of Sciences (in Chinese with English abstract).
Zhang, L., Bao, Z.D., Dou, L.X., Zang, D.S., Mao, S.W., Song, J., Zhao, J.H., Wang, Z.C., 2018. Sedimentary characteristics and pattern of distributary channels in shallow water deltaic red bed succession: a case from the Late Cretaceous Yaojia formation, southern Songliao Basin, NE China. J. Petrol. Sci. Eng. 171, 1171–1190.
Zhao, Z.Y., 1984. Structural pattern and evolution of Bohaiwan basin, China. Acta Pet. Sin. 5 (1), 1–8 (in Chinese with English abstract).
Zhao, X.Z., Jin, F.M., et al., 2012. Formation, Distribution and Fine Exploration of Reservoirs in Faulted Slope: Taking Jizhong Depression and Erlian Basin as Examples. Science Press, Beijing, pp. 1–200 (in Chinese with English abstract).
Zhao, M.F., Li, Y., Zhang, Y., Wang, D.P., 2006. Relation of cross-fault lithology juxtaposition and fault sealing. J. China Univ. Petrol. (Ed. Nat. Sci.) 30 (1), 7–11 (in Chinese with English abstract).
Zhao, X.Z., Jin, F.M., Zou, J., Hou, F.X., Dai, J.S., Sun, Z.H., 2014. Geological characteristics and hydrocarbon accumulation of weak tectonic zone in rift basin: geological characteristics and hydrocarbon accumulation of weak tectonic zone in rift basin: a case study from Jizhong depression. Nat. Gas Geosci. 25 (12), 1888–1895 (in Chinese with English abstract).
Zhu, X.Q., 2009. The Mantle Plume Model for the Evolution of Bohai Bay Basin. Degree's thesis. Yangtze University (in Chinese with English abstract). Degree's thesis. China University of Petroleum (EastChina) (in Chinese with English abstract).
Zhu, X.M., Zeng, H.L., Li, S.L., Dong, Y.L., Zhu, S.F., Zhao, D.N., 2017. Sedimentary characteristics and seismic geomorphologic responses of a shallow-water delta in the qingshankou formation from the songliao basin, China. Mar. Petrol. Geol. 79, 131–148.
Zou, J., Dai, J., Zhang, D., Wu, Y., Tian, B., 2014. Structural divisions of rift basin based on the intensity of tectonic activity: a case study from the Raoyang Sag. Acta Petrol. Sin. 35 (2), 294–302+384 (in Chinese with English abstract).